

2002

# Intramolecular C-H bond activation using cobalt complexes of constrained cyclam ligands

Thoi Dang Nguyen  
*San Jose State University*

Follow this and additional works at: [https://scholarworks.sjsu.edu/etd\\_theses](https://scholarworks.sjsu.edu/etd_theses)

---

## Recommended Citation

Nguyen, Thoi Dang, "Intramolecular C-H bond activation using cobalt complexes of constrained cyclam ligands" (2002). *Master's Theses*. 2368.

DOI: <https://doi.org/10.31979/etd.36c3-nquy>

[https://scholarworks.sjsu.edu/etd\\_theses/2368](https://scholarworks.sjsu.edu/etd_theses/2368)

This Thesis is brought to you for free and open access by the Master's Theses and Graduate Research at SJSU ScholarWorks. It has been accepted for inclusion in Master's Theses by an authorized administrator of SJSU ScholarWorks. For more information, please contact [scholarworks@sjsu.edu](mailto:scholarworks@sjsu.edu).

## **INFORMATION TO USERS**

**This manuscript has been reproduced from the microfilm master. UMI films the text directly from the original or copy submitted. Thus, some thesis and dissertation copies are in typewriter face, while others may be from any type of computer printer.**

**The quality of this reproduction is dependent upon the quality of the copy submitted. Broken or indistinct print, colored or poor quality illustrations and photographs, print bleedthrough, substandard margins, and improper alignment can adversely affect reproduction.**

**In the unlikely event that the author did not send UMI a complete manuscript and there are missing pages, these will be noted. Also, if unauthorized copyright material had to be removed, a note will indicate the deletion.**

**Oversize materials (e.g., maps, drawings, charts) are reproduced by sectioning the original, beginning at the upper left-hand corner and continuing from left to right in equal sections with small overlaps.**

**ProQuest Information and Learning  
300 North Zeeb Road, Ann Arbor, Mi 48106-1346 USA  
800-521-0600**

**UMI<sup>®</sup>**



**INTRAMOLECULAR C-H BOND ACTIVATION USING  
COBALT COMPLEXES OF CONSTRAINED CYCLAM  
LIGANDS**

**A Thesis**

**Presented to**

**The Faculty of the Department of Chemistry**

**San Jose State University**

**In Partial Fulfillment**

**of the Requirements for the Degree**

**Master of Science, Chemistry**

**by**

**Thoi Dang Nguyen**

**December 2002**

**UMI Number: 1411621**

**UMI<sup>®</sup>**

---

**UMI Microform 1411621**

**Copyright 2003 by ProQuest Information and Learning Company.  
All rights reserved. This microform edition is protected against  
unauthorized copying under Title 17, United States Code.**

---

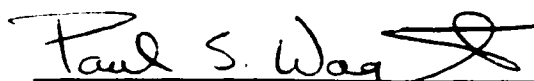
**ProQuest Information and Learning Company  
300 North Zeeb Road  
P.O. Box 1346  
Ann Arbor, MI 48106-1346**

© 2002

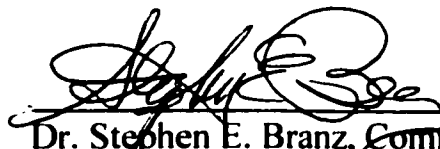
**Thoi Dang Nguyen**

**ALL RIGHTS RESERVED**

APPROVED FOR THE DEPARTMENT OF CHEMISTRY, SJSU



Dr. Paul S. Wagenknecht, Faculty Advisor

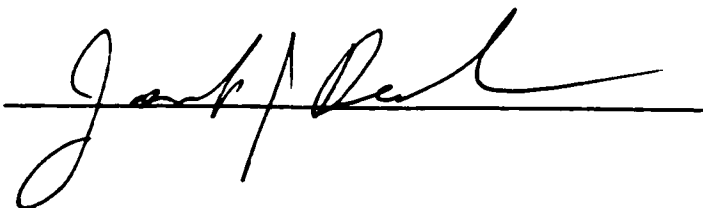


Dr. Stephen E. Branz, Committee Member



Dr. Maureen A. Scharberg, Committee Member

APPROVED FOR THE UNIVERSITY



## ABSTRACT

### INTRAMOLECULAR C-H BOND ACTIVATION USING COBALT COMPLEXES OF CONSTRAINED CYCLAM LIGANDS

By Thoi D. Nguyen

This study addresses the topic of intramolecular C-H bond activation by transition metal complexes. To study this activation, the syntheses and structural elucidations of two constrained ligands ( $H_2dc3$  and 1,11- $C_3$ -cyclam) and their corresponding cobalt complexes are carried out. The conditions leading to C-H bond activation are examined. Electrochemical study of  $Co(dc3)$  is carried out. In addition, the conditions required for the insertion of cobalt into 1,11- $C_3$ -cyclam are examined.

Using 2-D NMR experiments, the resonances of the  $^1H$  and  $^{13}C$  NMR spectra of  $Co(dc3)$  are assigned. The presence of a base causes the C-H bond tethered to cobalt in  $Co(dc3)$  to cleave in an electrophilic activation mode resulting in the formation of the Co-C bond. Electrochemical study of  $Co(dc3)$  implicates Co-C bond rupture upon one electron reduction. Since 1,11- $C_3$ -cyclam is highly basic, cobalt insertion into 1,11- $C_3$ -cyclam was carried out in aprotic anhydrous solvents. The isolated complex was determined to be  $[Co(1,11-C_3-cyclam)(NCS)_2]SCN$ .



## ACKNOWLEDGEMENTS

Besides having a vague dream of becoming a scientist, I did not set out to become a chemist. Luckily, many talented and dedicated people helped me to turn this vague dream into a reality and shaped me into who I am today. First and foremost, I am forever indebted to my parents who sacrificed for me and loved me unconditionally. No matter what I do, I could never render enough thanks. I am grateful to the dedication and patience of my advisor, Dr. Wagenknecht, who continued to encourage me despite my many unsuccessful experiments, and who taught me how to think critically and to write succinctly. He is truly a great teacher. I am thankful to Uyen-Nhi, my soul mate, for her commitment and belief in me. There is nothing in life that I could not share with her. I am appreciative for the friendship of Dr. Chuanjiang Hu and Vidhya Krishnamoorthi. You two made my day a little bit better. I am grateful to Dr. Branz and Dr. Scharberg for their love of teaching and for their care for students. Last but not least, I would like to thank Dr. Chichester, Dr. Stacks, and the chemistry department staff for making my teaching apprenticeship here an enjoyable experience. I will cherish the time I worked and studied at San Jose State for the rest of my life.

## Table of Contents

List of Figures	IX
List of Tables	XI
<b>Chapter 1: Introduction to Alkane Transformations via C-H Bond Activation</b>	<b>1</b>
1.1 The Importance of Alkane Transformations	2
1.2 Chemical Properties of Alkanes	3
1.3 Activation and Functionalization of C-H Bonds of Alkanes by Biocatalysts	4
1.3.1 Cytochrome P450	4
1.3.2 Methane Monooxygenase	9
1.4 Pathways to the Transformations of Alkanes via C-H Bond Activation	11
1.4.1 Theoretical Aspects of C-H Bond Activation	11
1.4.2 Alkane Activation Using Metal Atoms and Ions	12
1.4.2.1 Alkane Activation by Metal Atoms	12
1.4.2.2 Alkane Activation Using Metal Ions in the Gas Phase	13
1.4.3 Alkane Activation by High-valent Metal Complexes	15
1.4.4 C-H Bond Activation Mediated by Low-valent Transition Metal Complexes	17
1.4.4.1 The Question of Intermolecular vs. Intramolecular C-H Bond Activation	20

1.5	Case Study: Intramolecular C-H Bond Activation in the Co(dacoda) Complex	24
1.6	Previous Work in Our Group	26
1.6.1	Co(dc3) Synthesis	27
1.6.2	Attempts to Break the Co-C Bond by Adding Triflic Acid	30
<b>Chapter 2: Further Study of the Co(dc3) Complex</b>		31
2.1	Introduction	32
2.2	Experimental	33
2.2.1	Materials and Methods	33
2.2.2	Synthesis of Co(dc3)	34
2.2.3	Reduction of Co(dc3) by Bis(cyclopentadienyl)cobalt	34
2.3	Results and Discussion	35
2.3.1	The Effect of KH on Co(dc3) Formation	35
2.3.2	NMR Experiments	36
2.3.3	Electrochemistry of Co(dc3)	40
2.3.4	Attempts to Chemically Reduce Co(dc3) by Bis(cyclopentadienyl)cobalt	43
<b>Chapter 3: Synthesis and Characterization of a New Constrained Tetraaza-macrocycle; Its Metallation and Protonation Reactions</b>		45
3.1	Introduction	46
3.2	Experimental	47
3.2.1	Materials and Methods	47

3.2.2	Synthesis of 1,11-C <sub>3</sub> -cyclam	47
3.2.3	Attempts to Synthesize [Co(1,11-C <sub>3</sub> -cyclam)(NO <sub>2</sub> ) <sub>2</sub> ]ClO <sub>4</sub>	48
3.2.4	Synthesis of [Co(1,11-C <sub>3</sub> -cyclam)(NCS) <sub>2</sub> ]SCN	49
3.3	Results and Discussion	50
3.3.1	1,11-C <sub>3</sub> -cyclam Synthesis and Reactivity	50
3.3.2	Synthesis of [Co(1,11-C <sub>3</sub> -cyclam)(NCS) <sub>2</sub> ]SCN	57
3.4	Conclusion	58
	<b>References</b>	60
	<b>Appendix 1</b> Additional Figures and NMR Spectra for Chapter 1	63
	<b>Appendix 2</b> Additional NMR Spectra for Chapter 2	68
	<b>Appendix 3</b> Additional Figure and NMR Spectra for Chapter 3	71

## List of Figures

Figure	Title	
1.1	Ferric heme thiolate catalytic center of cytochrome P450	5
1.2	Proposed radical mechanism of alkane hydroxylation by cytochrome P450	7
1.3	Proposed agostic mechanism for alkane hydroxylation by cytochrome P450	8
1.4	Catalytic cycle of MMO	10
1.5	Molecular orbital diagram for alkanes	12
1.6	Reaction of cyclohexane with a nickel complex	14
1.7	Activation of butane by Ni(I)	14
1.8	Mechanism for the activation and functionalization of C-H bonds by high-valent metal complexes	15
1.9	Chromyl-oxo reagent catalyzes the activation of C-H bonds in alkanes	16
1.10	Modes of C-H bond activation, oxidative addition, and electrophilic cleavage	18
1.11	Activation of the C-H bond of benzene by the bis(1,2-dimethyl-phosphinoethane)ruthenium dichloride complex	21
1.12	Activation of C-H bonds of hydrocarbon solvents by $(\eta^5\text{-C}_5(\text{CH}_3)_5)\text{IrH}_2\text{P}(\text{CH}_3)_3$	23
1.13	Intramolecular vs. intermolecular oxidative addition	23
1.14	Intramolecular C-H bond activation by Co(dacoda) complex	25
1.15	Examples of strapped tetraazamacrocyclic, H <sub>2</sub> dc3 and 1,11-C <sub>3</sub> -cyclam	27
1.16	Preparation of H <sub>2</sub> dc3	27

1.17	Synthesis of Co(dc3)	28
1.18	Deprotonation of the agostic C-H by a base	28
1.19	Attempt to break the Co-C bond by triflic acid	30
2.1	Co(dc3)	38
2.2	Electron diagram of Co(dc3)	40
2.3	Possible electron diagram of Co(II) complex	41
2.4	The rupture of the Co-C bond	41
2.5	Cyclic voltammogram of Co(dc3)	42
2.6	The rupture of a Co-C bond in Cobalamin by reduction of Co(III) to Co(II)	43
3.1	The preparation of 1,11-C <sub>3</sub> -cyclam from H <sub>2</sub> dc3	46
3.2	Possible routes for the synthesis of 1,11-C <sub>3</sub> -cyclam	50
3.3	Possible byproducts for the bridging alkylation of cyclam	51
3.4	1,11-C <sub>3</sub> -cyclam	52
3.5	Formation of [H <sub>2</sub> 1,11-C <sub>3</sub> -cyclam](ClO <sub>4</sub> ) <sub>2</sub>	53
3.6	Structure of proton sponge (1), 1,11-C <sub>3</sub> -cyclam (2), 1,8-diazabicyclo[6.3.3]tetradecane (3), and 11-methylene-1,5,9-triazabicyclo[7.3.3.]pentadecane (4)	55

## List of Tables

<b>Table</b>	<b>Title</b>	
2.1	The effect of using different equivalents of KH on the Co(dc3) yield	35
3.1	pK <sub>a</sub> of protonated amines	56

**Chapter 1: Introduction to Alkane Transformations via C-H  
Bond Activation**



## 1.1 The Importance of Alkane Transformations

The petrochemical industry each year uses millions of tons of petroleum and natural gas as a source of raw material for the mass production of many valuable organic materials. Examples of this large scale production are the production of methanol and ethylene. In 1999, the U.S. chemical industry produced 6 million tons of methanol.<sup>1</sup> Even more important than the production of methanol is the production of ethylene which currently reaches 24 million tons annually. Overall, 46% of natural gas is used to produce petrochemicals.

To produce this quantity of petrochemicals, the chemical industry relies on brute force approaches of applying very high temperature and very high pressure to carry out the syntheses. The following reaction requires such extreme reaction conditions.



In this reaction, methane is oxidized at 350 °C and 300 atm in the presence of zinc oxide to yield methanol. These conditions obviously require tremendous energy input. Certainly under these reaction conditions, chemical selectivity for the conversion of longer chain alkanes to alcohols can hardly be achieved. Recognizing the disadvantages of these chemical processes, the chemical industry has been trying for years to find an innovative way of carrying out these basic chemical transformations under much milder reaction conditions. It would be preferable to have a reaction that can run at room temperature and atmospheric pressure. Reaching this goal would not only allow the

chemical industry to produce organic materials at a much reduced cost, but also would give new tools for chemists to carry out the functionalization of more complex alkanes with high control of chemical selectivity. Despite enormous effort of both the industrial and academic communities, this goal has not yet been realized due to the inherent properties associated with alkanes.

## **1.2 Chemical Properties of Alkanes**

Alkanes are usually the first group of organic compounds mentioned in undergraduate organic chemistry courses and are often referred to as unreactive; thus the term "paraffin" (affinity to little = parum affinis). In this section, only alkane properties that directly contribute to the inertness of alkanes as well as the task of C-H bond activation will be presented.

Since carbon and hydrogen both belong to the small group of elements that have the number of valence electrons equal to the number of valence orbitals available, alkanes consist of only C-H and C-C single bonds. They lack the electron pairs and empty orbitals necessary for polar reactions. Reactions of alkanes by a radical pathway are also hampered by the strong bonding between carbons or between carbon and hydrogen (bond dissociation energy for C-C bond ~ 80-90 kcal/mole and C-H bond ~ 90-104 kcal/mole).<sup>2</sup> The third factor that contributes partly to the inertness of alkanes is the low polarity of the C-H bond which makes alkanes much less susceptible to attacking reagents.

Determination of the reactivity of a compound based on its polarity, however, is not always consistent due to conflicting observations. Fluorocarbons, despite having very

polar bonds, are very inert. These three factors contribute mainly to the inertness of alkanes in typical reaction conditions.

Under extreme reaction conditions, alkanes are found to react with radicals, carbenes, super acids, and peroxide.<sup>3</sup> Unfortunately, products formed under these extreme conditions are often complex mixtures because of the high reactivity of the newly formed products when compared to the starting materials. Selective functionalizations of alkanes are therefore very difficult to attain.

Despite these inherent properties of alkanes that make them so hard to activate in a controlled manner, chemists continue to search for solutions to alkane functionalizations. Very often, in the long quest for this solution, they are inspired by glowing examples of biocatalysts that carry out C-H activation and alkane functionalizations with ease and great control.

### **1.3 Activation and Functionalization of C-H Bonds of Alkanes by Biocatalysts**

Many enzymes can carry out chemical transformations with ease and great selectivity. The degree of selectivity of most of these enzymes surpasses even the most cleverly designed artificial catalysts. However, these enzymes, having been tuned for million of years, are complex systems and only recently have scientists started to uncover some of the mysteries behind the mechanisms of these enzymes. In the field of C-H bond activation, two biocatalysts, cytochrome P450 and methane monooxygenase, serve as an inspiration for those who want to learn about C-H bond activation. In the following section, these two biocatalysts will be introduced briefly.

#### **1.3.1 Cytochrome P450**

Cytochrome P450 enzymes constitute a superfamily of heme-thiolate proteins and are widely distributed in bacteria, fungi, plants and animals. The enzymes are involved in the metabolism of a wide range of both exogenous and endogenous compounds. Usually, they act as terminal oxidases in multicomponent electron transfer chains, called here cytochrome P450 enzyme systems. In humans, the cytochrome P450 enzyme system can be found in the liver and carries out the hydroxylation of alkanes as a way to biotransform xenobiotics.<sup>4</sup>

The net reaction for alkane hydroxylation is shown below.



In the process of hydroxylation, cytochrome P450 first activates the C-H bond and in a subsequent step functionalizes the activated alkane.

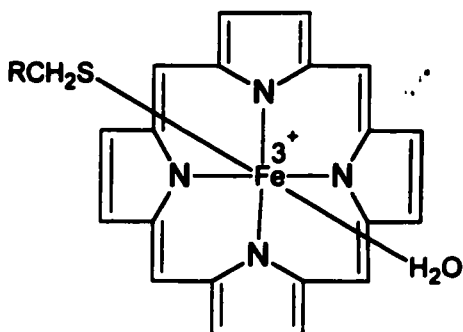


**Figure 1.1:** Ferric heme thiolate catalytic center of cytochrome P450.

It has been well accepted that the resting state of cytochrome P450 is not catalytically active. Rather, the resting state of cytochrome P450 must undergo a series of electron transfer processes which eventually lead to the formation of an active high-valent iron-oxo species. However, the structures of the intermediates in this electron transfer processes have not been established.<sup>4</sup> Recently, Hoffman and coworkers<sup>5</sup> used electron paramagnetic resonance (EPR) and electron nuclear double resonance (ENDOR) spectroscopies conducted at cryogenic temperatures to characterize the well-controlled multiple-step transformation from the resting state to the active state of cytochrome P450. Using this method, Hoffman and coworkers were able to identify the intermediates as well as the active species of the catalytic cycle of cytochrome P450. As a result, the active state of cytochrome P450 is determined to be the Fe<sup>IV</sup>oxo species. This high-valent iron-oxo species can then carry out the hydroxylation of hydrocarbons through a two-step mechanism, first with the activation of the C-H bond of the alkyl substrate and second with the functionalization of the activated alkane to form a new C-OH bond.

Although the overall mechanism is well understood, details of the C-H bond activation step are still controversial. It has been thought for a long time that the active form of the cytochrome P450 activates the C-H bond through a radical mechanism (Figure 1.2).<sup>6,7</sup> Since the iron-oxo species is highly electrophilic, it can abstract hydrogen from an inactivated alkane to give an alkyl radical and an iron-hydroxyl species. This alkyl radical then reacts with the iron-hydroxy species in a homolytic substitution reaction to yield an alcohol and return the resting state of cytochrome P450. Evidence supporting this step of the C-H bond activation mechanism through radical

abstraction on the C-H bond includes 1) the result of probe studies that give rearranged products consistent with radical intermediates<sup>6</sup> and 2) studies of the isotope effect.<sup>8</sup>

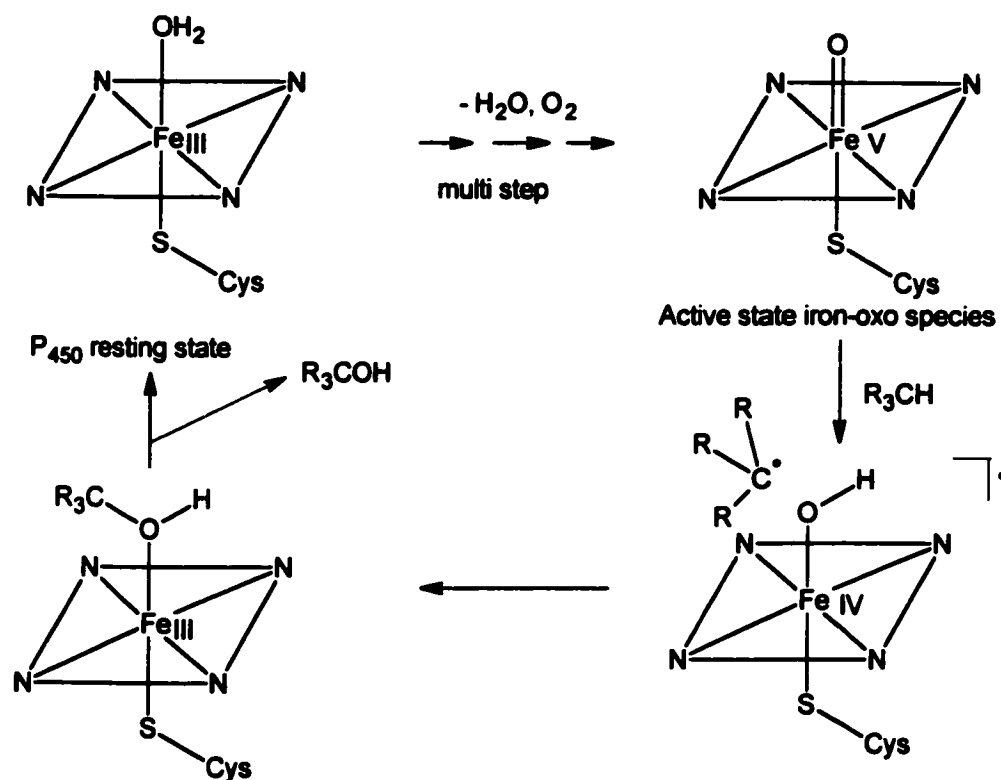


**Figure 1.2:** Proposed radical mechanism of alkane hydroxylation by cytochrome P450.

Recently, Newcomb and coworkers<sup>9</sup> used a technique called radical clock to test for the validity of the proposed radical mechanism of C-H bond activation in cytochrome P450. Since each alkyl radical has a certain lifetime, alkyl radicals formed in the catalytic reaction of probe substrates by cytochrome P450 should have the same lifetime as that of the controlled alkyl radicals. However, it was found that the lifetimes of the radicals formed in the catalytic reactions are *different* from the lifetimes of controlled

radicals. This result indicates that the C-H bond activation step may proceed by an alternative pathway.

Because of this new result Collman, Brauman, and coworkers<sup>10</sup> proposed an “agostic” mechanism (Figure 1.3) for the activation and functionalization of alkyl substrates by cytochrome P450. Here, the term “agostic” refers to the interaction of the C-H bond and the metal forming a three center two electron M-H-C bond (M = metal). According to this mechanism, the formation of an agostic substrate-catalyst complex is the key step in the hydroxylation of alkyl substrates. Due to the side-on interaction of the C-H bond with the d orbitals of the metal, the electron density from the C-H bond is distributed over three atom centers. Because of this distribution of electron density over more atoms, the Bronsted-Lowry acidity of the agostic hydrogen increases substantially. This allows the agostic hydrogen to migrate to the basic oxo group. Subsequent reductive elimination of the ROH group leads to the regeneration of the catalyst and the release of the alcohol.

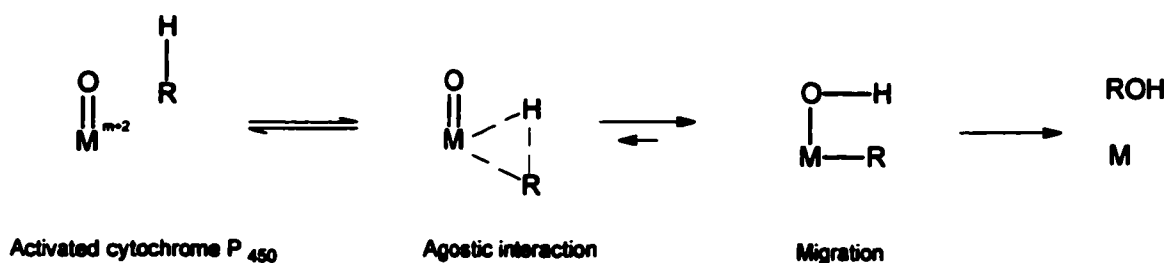


**Figure 1.3:** Proposed agostic mechanism for alkane hydroxylation by cytochrome P450.

To support this agostic mechanism, Collman, Brauman, and coworkers<sup>10</sup> carried out further experiments. They were able to prove that the hydroxylation reaction of the alkyl substrate by the iron-oxo species is inhibited by both the addition of dihydrogen and methane. Since substrates which form strong agostic complexes should inhibit the oxidation of more weakly bound substrates by sequestering the active catalyst and because methane and dihydrogen are known to form strong agostic complexes, the inhibition of hydroxylation of alkyl substrate by the addition of dihydrogen and methane supports the agostic mechanism for the C-H bond activation step.

The difference between the radical mechanism and the agostic mechanism for the C-H bond activation step is rather small if one looks at the overall proposed mechanism for the functionalizations of alkanes by cytochrome P450. One could even argue the benefit gained from studying such a small difference. However, this small difference represents a technical challenge that chemists need to understand before starting to construct a new catalytic system.

### **1.3.2 Methane Monooxygenase (MMO)**

In contrast to the widespread occurrence of cytochrome P450, MMO is found only in methanogenic bacteria.<sup>11</sup> The function of MMO in these bacteria is to oxidize methane into a useful source of carbon and in the process to provide energy for the bacteria. The net equation for this conversion is shown below.





In the above reaction, NAD(P)H is used to break the O=O bond of O<sub>2</sub>. One of the oxygen atoms of O<sub>2</sub> is used for the hydroxylation of methane to methanol and the other oxygen is reduced to water. Besides catalyzing the hydroxylation of methane, MMO can also catalyze the oxidation of a wide range of hydrocarbons such as saturated, unsaturated, linear, branched, and cyclic alkanes.<sup>11</sup>

Based on crystallographic studies, Rosenzweig et al.<sup>12</sup> determined that the oxidized form of MMO is a non-heme, diiron center compound. This oxidized form of MMO is also postulated as the active state. The mechanism for the activation and reduction steps of hydrocarbons by MMO is not as well understood as that of cytochrome P450. However, the key intermediates for MMO's catalytic process are known. Based on this, a mechanistic scheme is proposed<sup>11</sup> (Figure 1.4).

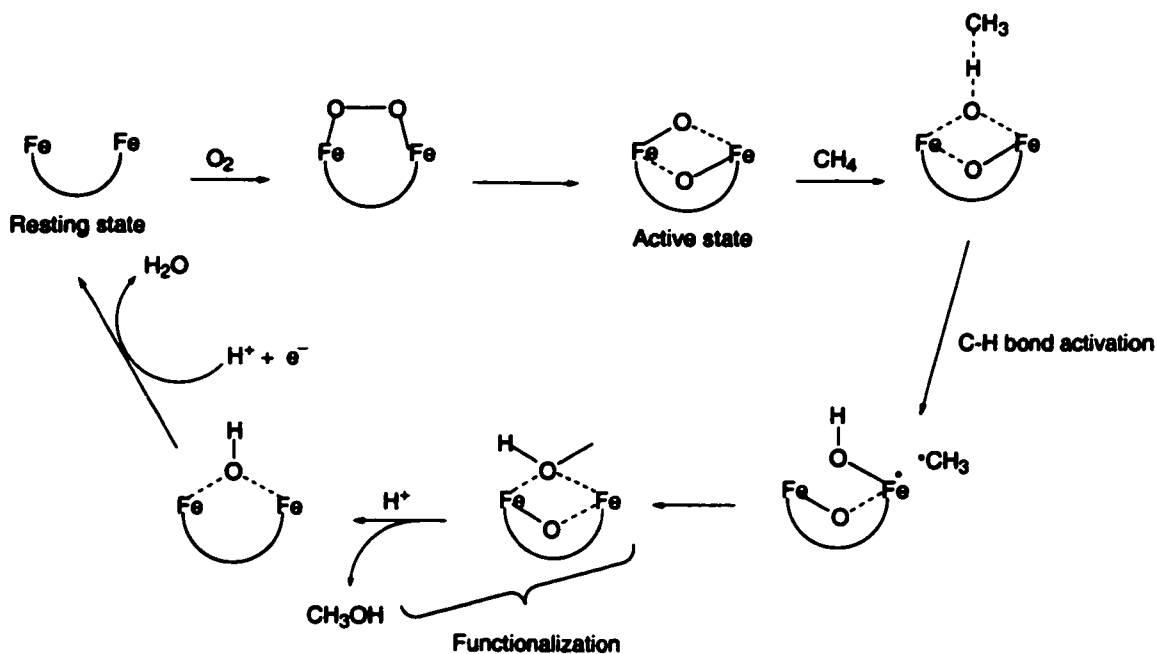


**Figure 1.4:** Catalytic cycle of MMO.

It has been proposed<sup>12</sup> that the catalytic step involves first the binding of alkyl substrates to the activated MMO through the oxygen bridging ligand. The abstraction of H from the alkyl/substrate results in a transient diradical. The alkyl radical in the subsequent step recombines with the oxenoid radical (in the bridging position) to form a covalently bound ROH ligand. Subsequently, the cleavage of the ROH ligand yields the alcohol and reforms the starting MMO.

#### **1.4 Pathways to the Transformations of Alkanes via C-H Bond Activation**

A great deal of information can be learned from the above enzymatic systems. However, replicating the above enzymatic systems seems to be a much more difficult task due to the complexity of these well-tuned biological systems. Rather, chemists look for systems that are much simpler in scope and are easy to control. In approaching the problem of C-H bond activation, we first need to understand the theoretical picture of how to break the C-H bond based on molecular orbital theory.

##### **1.4.1 Theoretical Aspects of C-H Bond Activation**

In order to weaken the C-H bond of alkanes, the C-H bond order needs to be lowered. To lower the bond order, an attacking reagent must either 1) donate electrons into the antibonding orbital 2) withdraw electrons from the bonding orbital or 3) carry out the above two strategies simultaneously.

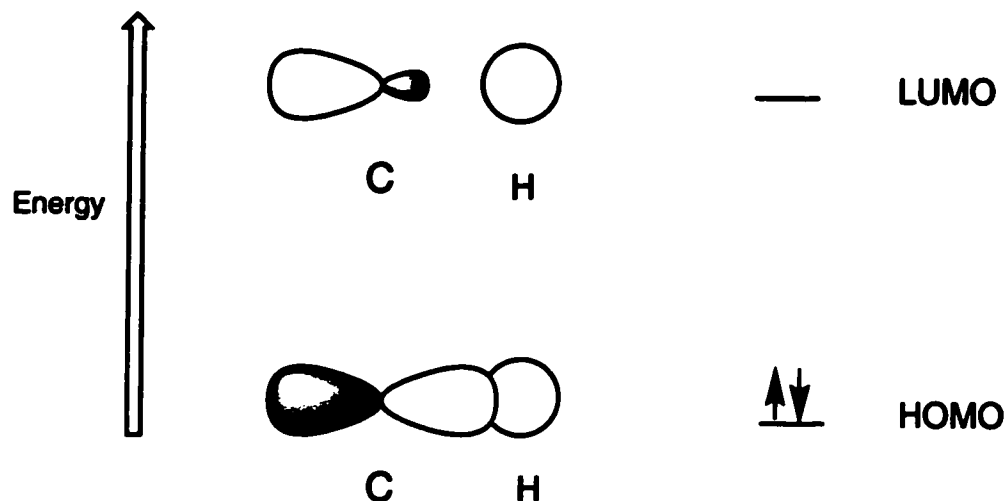


**Figure 1.5:** Molecular orbital diagram for alkanes.

Since nucleophiles do not react with alkanes, strategy 1) seems the least desirable approach. There are some known chemical reactions that can carry out C-H bond activation according to strategy 2. These examples include electrophilic reagents such as Lewis acids.<sup>13</sup> Strategy 3) seems to be the most successful since many reagents react with alkanes in this way. Those reagents includes: radicals, carbenes, metal surfaces, and metal complexes. In this section, the methods used to activate C-H bonds will be described in detail.

## **1.4.2 Alkane Activation Using Metal Atoms and Ions**

### **1.4.2.1 Alkane Activation by Metal Atom**

Many metals are known to have catalytic activity. The catalytic hydrogenation of olefins on a Pd surface is one fine example.<sup>2</sup> However, the use of metal *atoms* to carry out catalytic reactions is rarely observed. To observe this type of catalysis, metal vapor is

typically co-condensed at a cold surface with the substrate vapor. This co-condensation of the metal and the substrate allows the two species to interact at the molecular level. Interactions of metal and substrate that lead to catalytic activity require the rapid formation of strong metal substrate bonds. Otherwise, condensation of bulk metal predominates. The activation of C-H bonds according to this method was first observed by Klabunde.<sup>14</sup> In his experiment, nickel atoms were allowed to co-condense with pentane. Upon analyzing the composition of the deposit, the pentane carbons are found to rearrange such that C<sub>1</sub> forms a new bond with C<sub>5</sub>. This observation suggests that the metal atoms facilitate the cracking of the pentane and this cracking involves the activation of both C-H and C-C bonds.

Pearson,<sup>15</sup> in his attempt to elucidate the mechanism of this process, used Mossbauer spectroscopy to study the activation of methane. His result indicates the formation of an M-H intermediate which in turn indicates the successful activation of C-H bonds.

Research on C-H bond activation in this direction, however, is hampered by the inability to control the selectivity of the process. There are just too many by-products. Elucidation of the catalytic process is difficult to study due to the complexity associated with heterogeneous catalysts. In addition, the reaction conditions have to be controlled rigorously to exclude the possibility that a metal surface is the catalytic force behind alkane activation. Overall, the application of this new approach to industry is limited by many factors associated with the system.

#### **1.4.2.2 Alkane Activation Using Metal Ions in the Gas Phase**

The activation of alkanes can also be facilitated by a metal ion or a metal ion complex. Early experiments by Muller and Goll<sup>16</sup> showed that alkanes react with a metal ion complex to form an organometallic species.

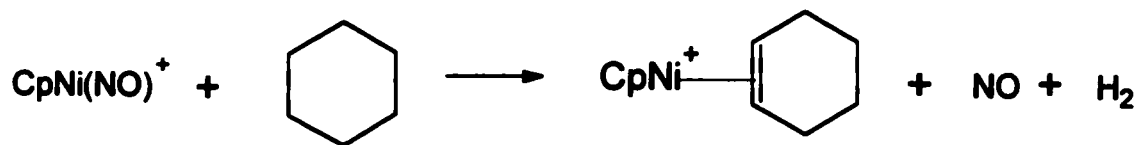


**Figure 1.6:** The reaction of cyclohexane with a nickel complex.

The formation of the organometallic species probably proceeds through a C-H bond activation step. Bare metal ions have also been found to activate alkanes.<sup>17</sup> Examples include the activation of both C-C bonds and C-H bonds by nickel ion (Figure 1.7).

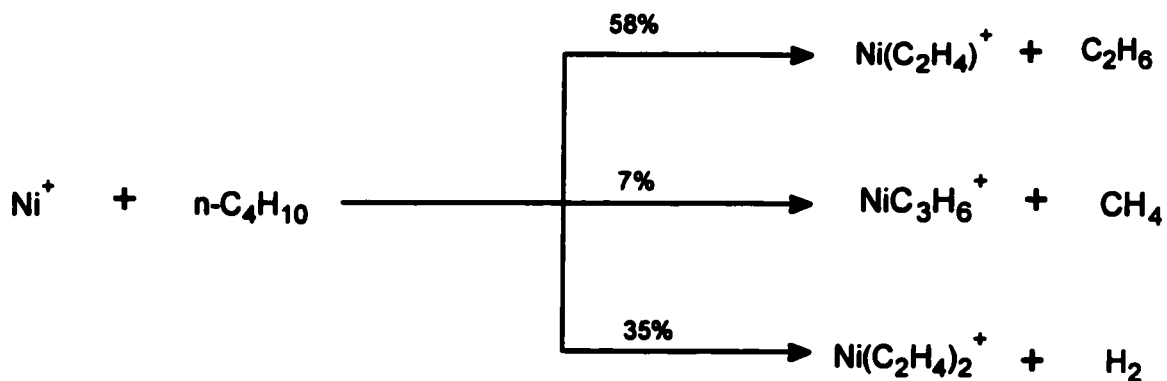


**Figure 1.7:** Activation of butane by Ni(I).

In this case, the metal ion can activate the C-C bonds and C-H bonds, a task that few homogeneous catalysts can do. This power of the metal ion in the activation of

alkanes can be explained by the bond strength of  $M-CH_3^+$  compared to  $M-H^+$ . For the case of the iron ion, Beauchamp<sup>17,18</sup> found that  $Fe-CH_3^+$  has a dissociation energy of 69.5 kcal/mol, 10 kcal greater than that of  $Fe-H^+$  (58.5 kcal/mol). Due to the formation of a more thermodynamically favorable intermediate, the metal ion can also facilitate scission of a C-C bond. Chemically, the activation of both C-H and C-C bonds decreases the selectivity of the reaction, thus activation of alkanes by metal ions is not valuable in industry.

### 1.4.3 Alkane Activation by High-valent Metal Complexes

Alkane activation by high-valent metal complexes constitutes a class which includes cytochrome P450 and methane monooxygenase. Since alkane activations by biocatalysts have been discussed previously, it is not presented here. Other routes for alkane activations by high-valent metal complexes include the use of iron complexes in the presence of strong oxidants such as  $O_2$  and peroxide to carry out alkane transformations (Figure 1.8).<sup>19</sup>

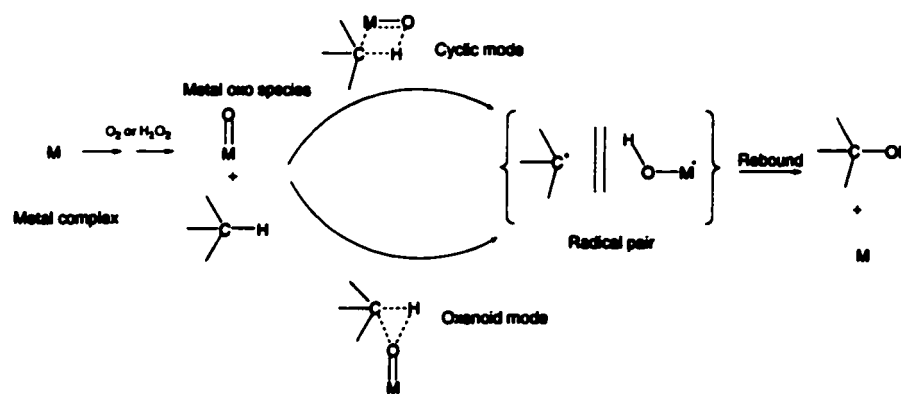


**Figure 1.8:** Mechanism for the activation and functionalization of C-H bond by high-valent metal complexes.

The function of adding such a strong oxidant is to form an in situ metal-oxo species. It is postulated that this in situ metal-oxo species is actually the active form that can facilitate H atom abstraction from the C-H bond through either an oxenoid mode or cyclic mode.

By either the cyclic or the oxenoid mode, the H atom abstraction results in the formation of a radical pair. This radical pair then undergoes a “rebound” step to yield an alcohol and to return the inactive starting metal complex. The formation of the metal-oxo species requires the metal to be high valent.

As an extension of this class, some catalysts in this group contain a stable metal-oxo bond in the starting material. This eliminates the need to synthesize the metal-oxo species in situ. Examples of these high-valent metal-oxo complexes include many widely used oxidants such as  $\text{CrO}_3$ ,  $\text{KMnO}_4$ , and  $\text{OsO}_4$ . Among these high-valent metal complexes containing the metal-oxo bond, the catalytic mechanism of chromyl-oxo reagents with the formula  $\text{CrO}_2\text{Y}_2$  ( $\text{Y} = \text{Cl}, \text{OAc}, \text{O}_2\text{CCF}_3$ ) have been studied the most due to their high solubility in organic solvents.<sup>19</sup> Presented in Figure 1.9 is the catalytic activation of C-H bonds in alkanes using a chromyl-oxo reagent (Figure 1.9).

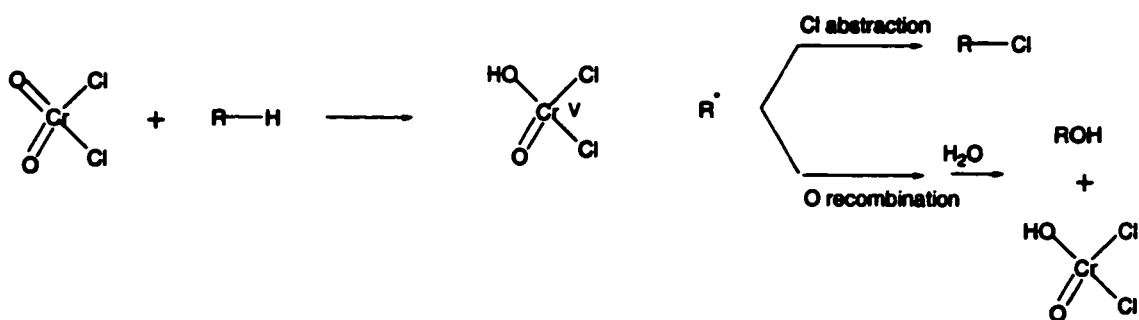


**Figure 1.9:** Chromyl-oxo reagent catalyzes the activation of C-H bonds in alkanes.

In this postulated mechanism, the hydrogen is first abstracted by a radical process to yield a carbon centered radical and a perchromic hydroxide. This step of the C-H bond activation was determined to be the rate determining step.<sup>19</sup> The driving force for this step and the overall reaction is the formation of the strong O-H bond in the chromyl moiety (80-85 kcal/mol) and the oxidation of Cr<sup>IV</sup> to Cr<sup>V</sup>.<sup>19</sup> The newly formed carbon-centered radical can either abstract the Cl from the chromium complex to form a halide or combine with the hydroxide of the chromium complex to form an alcohol.

Although the activation of C-H bonds by high-valent metal complexes have the advantage of using simple catalysts, they suffer heavily due to the low selectivity of the activation with linear, branched, and cyclic alkanes.<sup>19</sup> This low chemical selectivity makes it less appealing to industry.

#### **1.4.4 C-H Bond Activation Mediated by Low-valent Transition Metal Complexes**

C-H bond activation mediated by low-valent transition metal complexes have received great praise in the last thirty years because of the ability to carry out these catalytic reactions with high selectivity and because of the mild catalytic reaction conditions. Before going into details about the mode of catalysis, it is important to discuss the features that make this class of catalysts so desirable to industry.

As stated previously, the activation of C-H bonds requires either the withdrawal of electron density from the bonding orbitals of alkanes or the donation of electron density into the antibonding orbitals of alkanes or both. A transition metal complex can satisfy all these requirements for activation of a C-H bond. Due to having the same symmetry as the bonding orbital between the C and H of alkanes, an empty  $d_z^2$  orbital of



the metal in a coordination compound can withdraw electron density from the bonding orbitals between the C and H of alkanes. Simultaneously, the filled  $d_{xz}$  orbital or  $d_{yz}$  orbital of the metal can donate electron density back into the C-H antibonding orbitals. These two interactions reduce the bond order of alkanes. If these two interactions are strong enough, they lead to scission of the C-H bond.

For a catalyst to carry out the activation of C-H bonds, first and foremost, the d orbitals of the metal complexes must be able to interact with the orbitals of alkanes. Schematically, this interaction and its result can be described as follows (Figure 1.10).

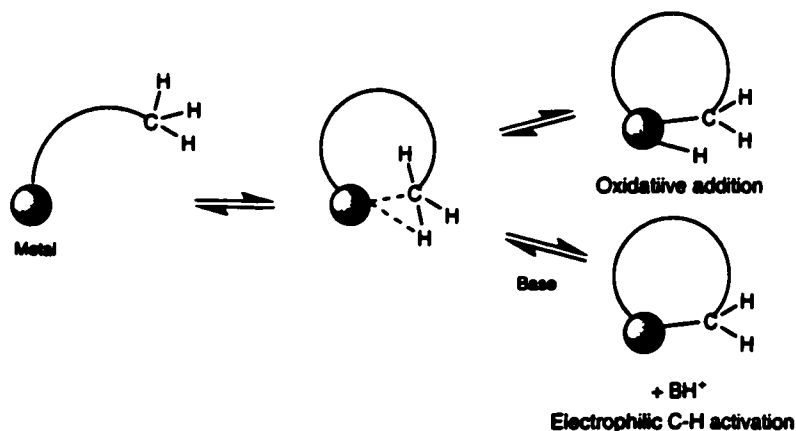


**Figure 1.10:** Modes of C-H bond activation, oxidative addition and electrophilic cleavage.

Here, for the purpose of simplifying the presentation, the alkane being activated is tethered to the metal center through some functionality. In a later section, I will compare and contrast both the tethered and untethered alkanes. Due to  $\sigma_{\text{alkane}} \rightarrow d_z^2_{\text{metal}}$  the two electrons from the C-H bond are extended over three atom centers. This interaction is known as a 3-center, 2-electron bond. The geometric features of this intermediate may

comprise an initial linear M-H-C interaction.<sup>20a</sup> There are many good examples of coordination complexes that have this almost linear M-H-C interaction (see Appendix 1). To proceed to bond cleavage, the M-H-C 3-center, 2-electron bond must rearrange into a three center cyclic intermediate. The formation of this cyclic intermediate has been extensively studied.<sup>3,20a,23</sup> In many mechanistic studies, this cyclic intermediate has been found to be the intermediate prior to the C-H bond cleavage.<sup>20b,20c,20d</sup> In one case, this intermediate has been isolated and studied by X-ray diffraction.<sup>21</sup>

A direct result of this cyclic interaction is the observation that the acidity of the proton in the M-H-C 3-center, 2-electron bond increases significantly when compared to the acidity of unactivated alkanes.<sup>3,20a,23</sup> This increase in acidity is the result of the depletion of electron density from the C-H bonding orbital. The depletion of electron density renders the H more electrophilic. A base can be used to deprotonate this C-H bond leading to the complete scission of the C-H bond and the formation of a new M-C bond. This mode of activation is termed "electrophilic C-H bond activation."

Alternatively, C-H bond activation can occur through oxidative addition. The term "oxidative" refers to the oxidation of the metal center while the term "addition" refers to the increase in coordination number of the metal complex after the scission of the C-H bond. In this mode, the two electrons from the 3-center, 2-electron bond and two electrons from the filled d orbitals of the metal are being used to form a new M-H bond and a new M-C bond. The metal is oxidized from n to n+2.

The driving force for C-H bond activation through both an electrophilic pathway or oxidative addition is the formation of new bonds. For electrophilic C-H bond

activation, a new M-C bond and a bond between the base and H<sup>+</sup> form. One M-H and one M-C bond are formed in the oxidative addition mode.

Given these two possible routes for C-H bond activation, one may ask what the dominant pathway is for a given set of reaction conditions? Since each of these pathways result in the formation of two new bonds and the bond strength of these new bonds are of the same order, it is more useful to talk about an allowed pathway than to discuss about a dominant pathway. Electrophilic C-H bond activation needs the presence of a base. Oxidative addition requires at least two open coordination sites. In addition, because of the need of the oxidative addition pathway to use the d electrons of the metal to form new bonds, electron rich metals are more likely to follow the oxidative addition pathway than electron poor metals.

#### **1.4.4.1 The Question of Intermolecular vs. Intramolecular C-H Bond Activation**

C-H bond activation by low-valent metal complexes can follow either an oxidative addition or the electrophilic pathway. Another aspect pertaining to C-H bond activation is that of intermolecular C-H bond activation vs. intramolecular C-H bond activation.

The first observation of C-H bond activation by the oxidative addition pathway was that of Chatt and Davidson in 1965.<sup>24</sup> It was observed that the reduction of the octahedral bis (1,2-dimethylphosphino-ethane) ruthenium dichloride complex in the presence of benzene gave the phenyl ruthenium hydride complex (Figure 1.11).

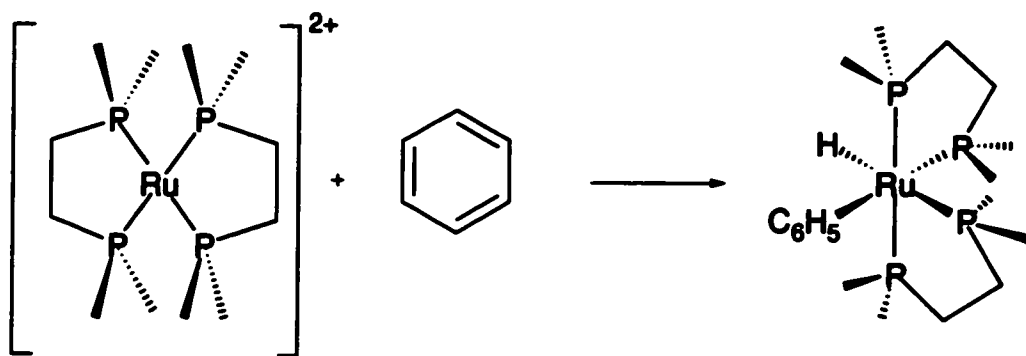


**Figure 1.11:** Activation of the C-H bond of benzene by the bis (1,2-dimethyl-phosphinoethane) ruthenium dichloride complex.

The formation of this phenyl ruthenium hydride complex implies that somehow, the starting complex facilitates the cleavage of the C-H bond in benzene, one of the strongest known C-H bonds. Following this report, many other systems capable of the activation of C-H bonds were reported. The majority of these systems involved intramolecular C-H bond activation.<sup>20,25</sup> Examples of some systems capable of intramolecular C-H activation are shown in Appendix 1.

In these systems, the C-H bonds being activated are associated with one of the ligands of the metal complex. The geometry of the ligand allows the C-H bond to closely approach the metal center. In other extreme cases, the C-H bond is forced by the constrained nature of the ligand to interact with the metal.<sup>21</sup> The close proximity becomes a dominant factor in imposing the interaction of the C-H bond and the metal, thus leading to C-H bond activation. Additionally, intramolecular C-H bond activation is also favored entropically over intermolecular C-H bond activation.<sup>20</sup> This entropic factor can be explained by comparing the number of reactants and products for each case. In

intramolecular C-H bond activation, one reactant molecule forms one product molecule. Whereas, in intermolecular C-H bond activation, two reactant molecules combine to form one product molecule.

Although, studying intramolecular C-H bond activation gives us valuable information about the conditions required to activate the C-H bond, a catalyst must be able to carry out intermolecular C-H bond activation to be useful industrially. Learning from the original system of Chatt and Davidson,<sup>24</sup> researchers realized that intermolecular C-H activation can only be carried out if there is no intramolecular C-H activation.<sup>20</sup> This means that the internal C-H bond (if there is any) must be kept away from the metal center. Also, there must be an open coordination site for the substrate to approach the metal. The use of a large metal center also facilitates the C-H bond activation because larger metals give stronger M-C and M-H bonds.

Applying these concepts in the early 1980s, researchers discovered new systems capable of catalyzing intermolecular C-H bond activation. Bergman and Janowicz<sup>26,27</sup> were the first group to discover intermolecular C-H bond activation of a saturated hydrocarbon (and its reverse) by using molecular iridium and rhodium complexes. Upon irradiation of  $(\eta^5\text{-C}_5(\text{CH}_3)_5)\text{IrH}_2\text{P}(\text{CH}_3)_3$  in hydrocarbon solvents such as neopentane or cyclohexane, they were able to isolate the alkyl-iridium hydride complexes (Figure 1.12).

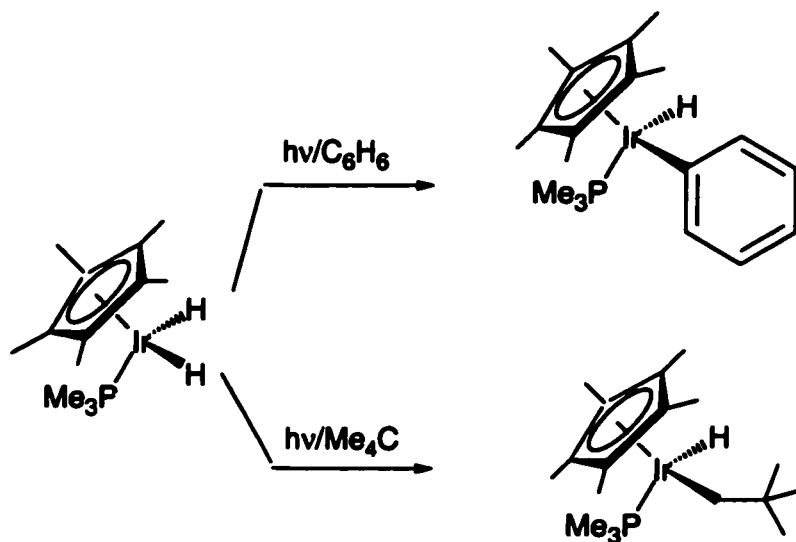


**Figure 1.12:** Activation of the C-H bond of hydrocarbon solvents by  $(\eta^5\text{-C}_5(\text{CH}_3)_5)\text{IrH}_2\text{P}(\text{CH}_3)_3$ .

In another experiment, Bergman and Janowicz demonstrated the competition between internal oxidative addition and external oxidative addition (Figure 1.13).

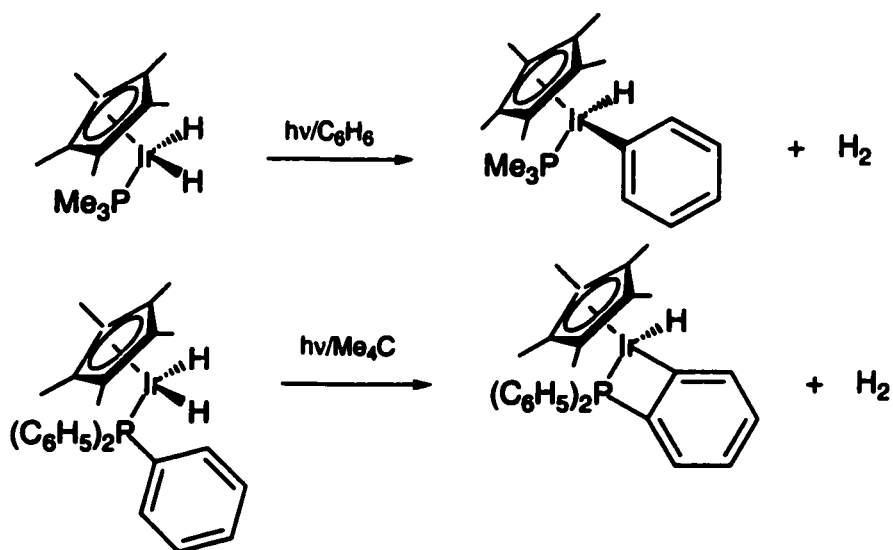


**Figure 1.13:** Intramolecular vs. intermolecular oxidative addition.

As shown above in the iridium complex with triphenylphosphine as a ligand, intramolecular oxidative addition predominates over the intermolecular mode because the C-H bond in the ortho position of the internal benzene is imposed to interact with the metal, thus forming the more favorable product. Whereas, with the use of similar ligands such as trimethyl phosphine, the internal oxidative addition cannot win over external oxidative addition because the C-H bonds of the  $\text{PMe}_3$  are not able to reach across and interact with the metal.

Many other desirable features of this system are also realized. The  $\eta^5\text{-C}_5(\text{CH}_3)_5$  ligand is a good donor, yet its methyl groups are too far away to interact with the metal. The alkyl phosphine is a good donor. And Ir metal complexes provide plenty of robustness (Ir is a 5d metal  $\rightarrow$  formation of much stronger Ir-alkyl and Ir-H bonds).

Soon after the discovery of such a robust system for C-H bond activation by Bergman and Janowicz, Jones and Feher<sup>28</sup> showed that the rhodium analogue of the Ir complex is capable of carrying out intermolecular C-H bond activation, despite some drawbacks such as the low stability of the resulting alkyl rhodium hydride complex. Hogano and Graham<sup>29</sup> showed that the photolysis of  $\eta^5\text{-C}_5(\text{CH}_3)_5\text{-Ir}(\text{CO})_2$  in cyclohexane produces a five coordinate complex  $\eta^5\text{-C}_5(\text{CH}_3)_5\text{IrH}(\text{cyclohexyl})\text{CO}$ . These new discoveries ushered in a new era of alkane activation catalyzed by homogenous catalysts.

### **1.5 Case study: Intramolecular C-H Bond Activation in the Co(dacoda) Complex**

With the discovery in the early 1980s of many systems capable of performing both intermolecular and intramolecular C-H bond activation, new venues have been opened leading to the ultimate goal of applying these discoveries industrially. At the

same time, it is also crucial to learn more about the mechanistic pathways leading to the activation of C-H bonds. Although early investigations into the mechanism of C-H bond activation have succeeded in providing a correct description of the process based on many indirect proofs<sup>30</sup> and experiments carried out at very low temperatures,<sup>31</sup> facile experiments proving this mechanism are lacking. The difficulty of detecting the fleeting M-H-C intermediate in intermolecular C-H activation largely reflects the fact that alkanes are poor ligands (no lone electron pair), and thus do not form stable complexes. Ideally, evidence for the mechanism of C-H bond activation would include 1) isolation of an intermediate metal-alkane complex and 2) a demonstration that this intermediate can proceed on to a system where the C-H bond has been cleaved. One way to make a more stable 3 center 2 electron M-H-C complex is to tether the C-H bond to the metal complex and to hold it in close proximity to the metal. A C-H bond can be held in close proximity to the metal by structural constraint.

Using Co(dacoda) (1, Figure 1.14), Legg and coworkers<sup>21</sup> have an isolated case where they have demonstrated the mechanism of C-H bond activation.

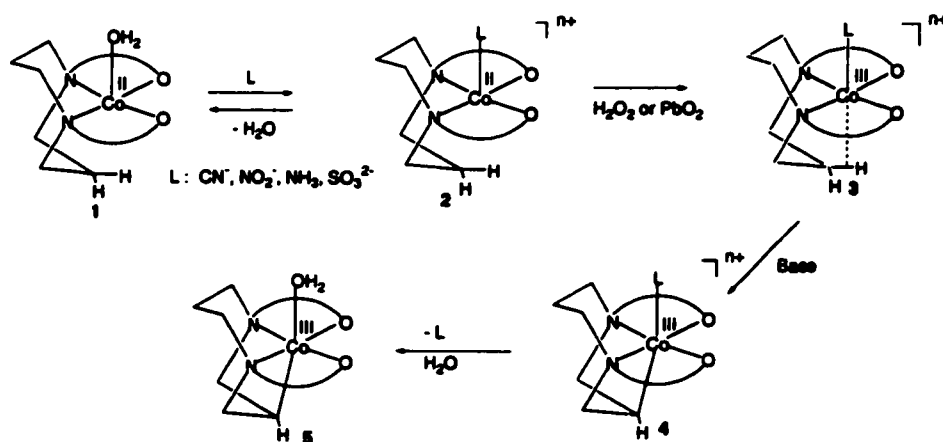


**Figure 1.14:** Intramolecular C-H bond activation by Co(dacoda) complex.



In this experiment, the water ligand from **1** is replaced by a higher-field ligand in **2**. This replacement is necessary because the presence of the higher field ligand in **2** allows a more facile oxidation of  $\text{Co}^{\text{II}}$  to  $\text{Co}^{\text{III}}$ . This  $\text{Co}^{\text{III}}$  complex is isolable and its structure has been determined by X-ray diffraction.<sup>21</sup> The crystal structure shows that **3** has a three membered cyclic Co-H-C bond. In this agostic interaction, the H in the M-H-C bond becomes more acidic. A base was added to deprotonate this Co-H-C bond in an electrophilic C-H activation pathway. The complex now has a new Co-C bond. This experiment shows a stepwise mechanism for C-H bond activation.

The successful delineation of this electrophilic C-H bond activation mechanism also provides two important points: the three carbon chain strapped to the backbone of the complex is long enough for the C-H bond to reach the metal center and the constraint of the two hydrocarbon straps provide additional force to hold the C-H bond in to place for interaction with the metal.

## **1.6 Previous Work in Our Group**<sup>32</sup>

Our group is also interested in studying the conditions required for C-H bond activation. Specifically, we want to learn about the effect on C-H bond activation caused by varying the electronic structure of the cyclic ligand.

Using the same motif as the Legg experiment,<sup>21</sup> we plan to utilize the constraint of two three-carbon straps attached to the amine backbone to induce an interaction between the C-H bond and an incorporated metal. To study the electronic effects of the ligand on C-H bond activation, we have devised a class of strapped tetraazamacrocycles

(Figure 1.15). These strapped tetraazamacrocycles should serve as good probes in studying intramolecular C-H bond activation.

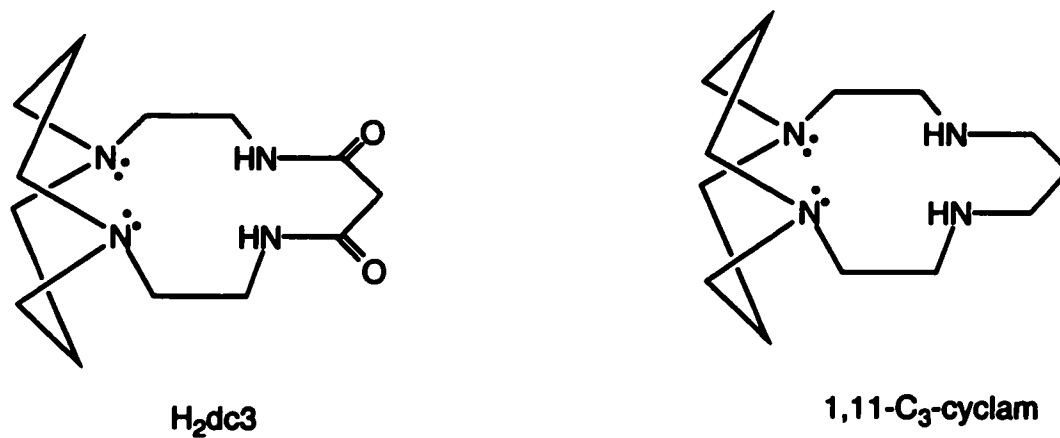


**Figure 1.15:** Examples of strapped tetraazamacrocycles, H<sub>2</sub>dc3 and 1,11-C<sub>3</sub>-cyclam.

Chin et al.<sup>32</sup> previously synthesized H<sub>2</sub>dc3 from dioxocyclam (Figure 1.16).

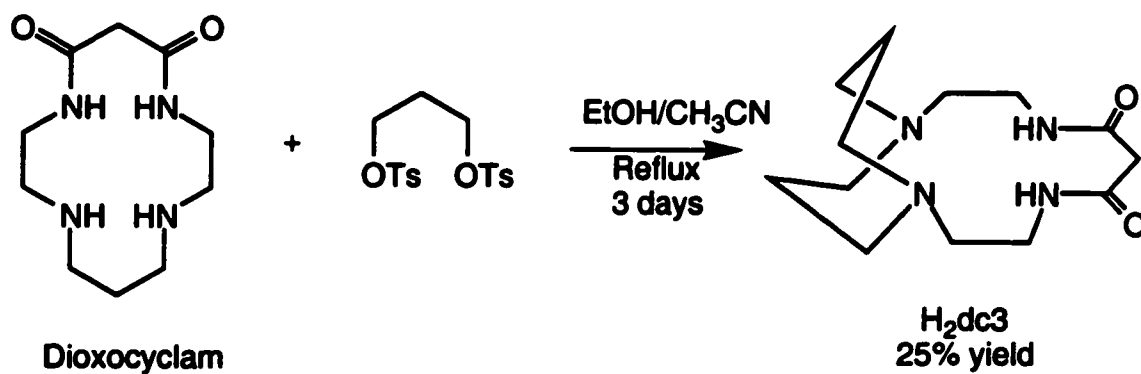


**Figure 1.16:** Preparation of H<sub>2</sub>dc3.

In this reaction, H<sub>2</sub>dc3 is the main product because the lone pairs of the amide nitrogens are not available for nucleophilic attack.

### 1.6.1 Co(dc3) Synthesis

Using similar ideas as Legg et al.,<sup>21</sup> Chin attempted to synthesize the cobalt(III) complex of H<sub>2</sub>dc3 in which the C-H bond has not been activated, but could only isolate the complex where the central C-H bond of the strap had been activated (Figure 1.17).<sup>32</sup>

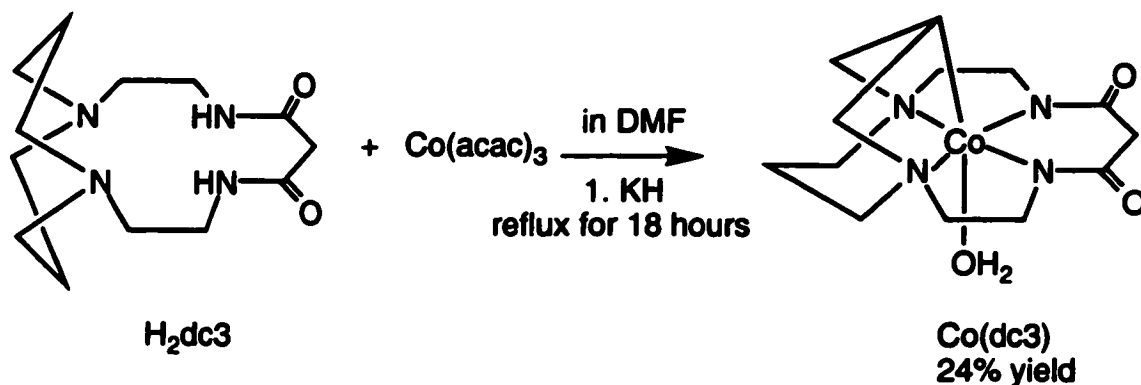


**Figure 1.17:** Synthesis of Co(dc3).

Although the purpose of adding potassium hydride was to deprotonate the two protons attached to the amide nitrogen of H<sub>2</sub>dc3, apparently the hydride also deprotonated the agostic C-H according to the following mechanism (Figure 1.18).

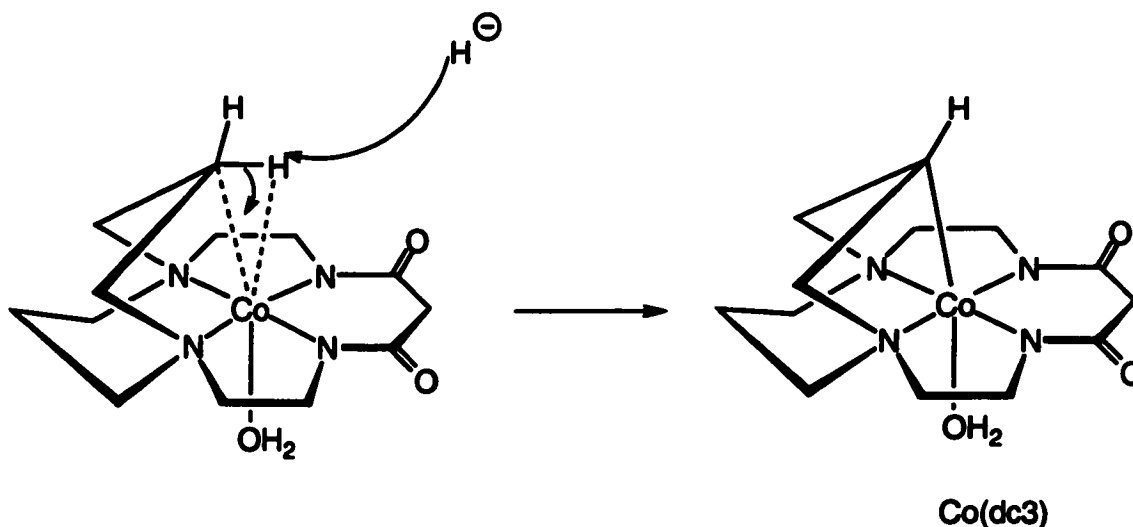


**Figure 1.18:** Deprotonation of the agostic C-H by a base.

Apparently, the C-H bond at the tip of the straps is induced to interact with the metal in an electrophilic C-H bond activation pathway as described previously. Due to this interaction, the H of the Co-H-C moiety becomes much more acidic compared to regular alkyl substrates. Since there is present a strong base (potassium hydride), this base can also deprotonate the agostic C-H. Deprotonation yields the Co(dc3) species with a novel Co-C bond. It should be noted that potassium hydride alone does not deprotonate unactivated alkanes.

Structural characterization of the Co(dc3) complex was performed primarily by NMR spectroscopy and X-ray diffraction. The crystal structure confirms the presence of the Co-C bond (distance between cobalt and carbon is 1.97 Å). In this case, the distance between cobalt and carbon is 0.04 Å longer than the combined covalent radius of cobalt and carbon. However, this difference has often been observed even for a true covalent bond between two nonmetals.<sup>2</sup> Therefore, the bond length of 1.97 Å between cobalt and carbon indicates a strong Co-C bond that probably has more covalent character than ionic character. The formation of this Co-C bond also breaks up the symmetry of the compound, i.e: the coordination plane is not a plane of symmetry.

Analysis of Co(dc3) by <sup>1</sup>H and <sup>13</sup>C NMR spectroscopy (Appendix 1) is hampered by the complexity of this system. It should be noticed that since the horizontal plane of symmetry has been destroyed, the atoms on one side of the N<sub>4</sub> plane of the molecule no longer experience the same chemical environment as the atoms below that plane; thus they are chemically inequivalent.

Using  $^{13}\text{C}$  NMR spectroscopy, Chin was only able to assign three of the eight signals.<sup>32</sup> Assigning the rest of the spectrum is difficult. The  $^1\text{H}$  NMR is even more difficult to assign and suggested that two dimensional NMR techniques would be necessary.

### 1.6.2 Attempts to Break the Co-C Bond by Adding Triflic Acid<sup>32</sup>

Since the purpose is to learn of the conditions leading to C-H bond activation and the product prepared by Chin et al.<sup>32</sup> already contained the Co-C bond resulting from C-H bond activation, it would be a good idea to try to break the Co-C bond so that its formation could subsequently be studied. Chin et al. reasoned that addition of strong acid would break the Co-C bond and reform the C-H bond in the following fashion (Figure 1.19).

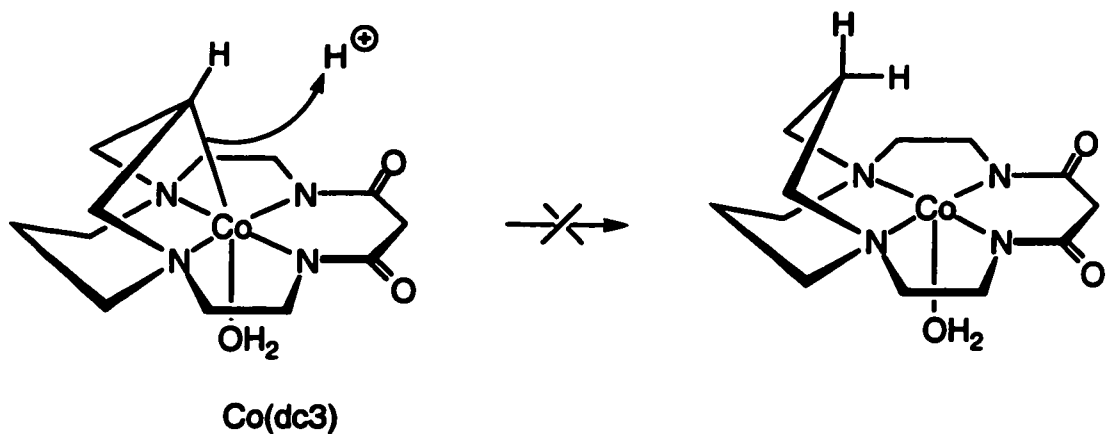


**Figure 1.19:** Attempt to break the Co-C bond by triflic acid.

The addition of triflic acid to a solution of  $\text{Co}(\text{dc}3)$ , however, resulted in no discernable change in the  $^1\text{H}$  NMR spectrum of the product. This observation probably reflects the strength of the Co-C bond, a point established earlier.

## **Chapter 2: Further Study of the Co(dc3) Complex**

## **2.1 Introduction**

The purpose of this project is to study the reaction conditions leading to intramolecular C-H bond activation as well as the mechanism of C-H bond cleavage. To study the mechanism of intramolecular C-H bond activation, we attempted to synthesize the cobalt(III) complex of H<sub>2</sub>dc<sub>3</sub> in which the C-H bond has not been activated, but could only isolate the complex in which the central C-H bond of the strap had been activated resulting in the formation of a Co-C bond. To study this reaction fully, we need to know what factors are involved in the formation of the Co-C bond as well as to fully analyze the compound by NMR spectroscopy. In addition, we need to look more into the possibility of using the existing Co(dc<sub>3</sub>) compound to study C-H bond activation.

In characterizing Co(dc<sub>3</sub>) by two dimensional NMR spectroscopy experiments, H-H correlation Spectroscopy (COSY) and Heteronuclear Correlation Spectroscopy (HETCOR) are performed. Combined with information obtained from the <sup>1</sup>H and <sup>13</sup>C NMR spectra, these 2-D experiments should provide a complete analysis of Co(dc<sub>3</sub>) by NMR spectroscopy.

The formation of Co(dc<sub>3</sub>) with a Co-C bond also challenges us to find a way to study the C-H bond activation process starting from the Co(dc<sub>3</sub>) complex. Previous attempts to break the Co-C bond by adding triflic acid were not successful. An alternative method is to cleave the Co-C bond by electrochemical methods. Lexa et al.,<sup>33</sup> Kim et al.,<sup>34</sup> and Huang et al.<sup>35</sup> demonstrated that the Co-C bonds in methylcobalamins, chemical systems that possess similar chemical environments as Co(dc<sub>3</sub>), can be cleaved by electrochemical methods. If the Co-C bond in Co(dc<sub>3</sub>) can be cleaved in this manner and

the C-H bond reformed, then perhaps the mechanism of C-H bond activation can be studied.

Additional benefits can be gained from the electrochemical study of Co(dc3). Since Co(dc3) possesses a similar chemical environment as that of cobalamins (four aza groups surrounding a cobalt center and a Co-C bond), electrochemical study of Co(dc3) can provide information about the potential usage of cobalt complexes of strapped cyclams as probes for studying cobalamins.

## **2.2 Experimental**

### **2.2.1 Materials and Methods**

H<sub>2</sub>dc3 was prepared by a slight modification of the literature procedure.<sup>36</sup> Instead of using 1M NaOH to dissolve the crude product, 2M NaOH was used. The product was then extracted with CH<sub>2</sub>Cl<sub>2</sub>. The CH<sub>2</sub>Cl<sub>2</sub> solvent was dried with MgSO<sub>4</sub> and filtered. The solvent was removed under reduced pressure. The resulting solid was then dissolved in CH<sub>3</sub>CN (25 ml) and the solution was filtered. The solvent was removed under reduced pressure. The resulting white solid was washed according to literature<sup>36</sup> to yield pure H<sub>2</sub>dc3.

For the synthesis of Co(dc3), basic alumina (activity I) was purchased and used as received. For obtaining cyclic voltammetry, LiClO<sub>4</sub> was dried by heating to 100°C under vacuum. All other materials were purchased and used as received. NMR spectra were recorded on a Varian INOVA 400 spectrometer. Chemical shifts were reported in ppm and referenced using the residual protonated solvent ( $\delta$  CD<sub>3</sub>OD 3.31 for <sup>1</sup>H NMR and 49.15 for <sup>13</sup>C NMR spectra). Cyclic voltammograms were obtained using a Bioanalytica



System CV-50W. An electrolysis cell was used with a 3.35 mm graphite disk working electrode, a saturated Ag/AgCl reference electrode, and a Pt-wire counter electrode.

### **2.2.2 Synthesis of Co(dc3)<sup>32</sup>**

In a drybox, H<sub>2</sub>dc3 (417.9 mg, 1.557 mmol) and KH (127.0 mg, 3.115 mmol) were placed in a 50 mL round bottom flask. DMF (6mL) was added to the mixture. The mixture was stirred for 15 minutes. Subsequently, Co(acac)<sub>3</sub> (400.0 mg, 1.556 mmol) was added as a solid to the KH/ H<sub>2</sub>dc3/DMF mixture. The vial was rinsed with 7 mL of DMF. The reaction mixture was brought out of the drybox and heated to 75-79°C for 18 hours. The reaction was cooled to room temperature and 9 mL of 2M NaOH was added to the mixture. The mixture was stirred for one hour. The solvent was removed under reduced pressure yielding a brown solid. This brown solid was chromatographed using basic alumina (1.3 cm × 30 cm). 200 mL of CH<sub>2</sub>Cl<sub>2</sub> was used initially to remove any unreacted Co(acac)<sub>3</sub>. The Co(dc3) was eluted with a 1:1 mixture of CH<sub>2</sub>Cl<sub>2</sub> and MeOH. The red band was collected, the solvent was removed and the resulting red solid was washed with 2 mL of H<sub>2</sub>O yielding 126.6 mg of Co(dc3) (Yield 24%). <sup>1</sup>H NMR data (CD<sub>3</sub>OD) δ 3.80 (m, 2H), 3.60 (m, 2H), 3.32 (s, 2H), 3.20 (m, 4H), 2.75 (m, 4H), 2.64 (m, 3H), 2.50 (d, 2H), 2.12 (b.s, 1H), 2.02 (d, 1H). <sup>13</sup>C NMR data (CD<sub>3</sub>OD) δ 176.69 (s), 64.79 (s), 61.07 (s), 55.67 (s), 45.92 (s), 45.67 (s), 25.13 (s), -10.53 (s). Anal. Calc. for C<sub>13</sub>H<sub>21</sub>CoN<sub>4</sub>O<sub>2</sub>·4H<sub>2</sub>O C, 39.38; H, 7.30; N, 14.14. Found: C, 39.47; H, 7.19; N, 14.03.

### **2.2.3 Reduction of Co(dc3) by Bis(cyclopentadienyl)cobalt**

Co(dc3) (10 mg, 0.029 mmol) was dissolved in 2 mL of MeOH. To this solution, Bis(cyclopentadienyl)cobalt (5.5 mg, 0.029 mmol) was added. The mixture was stirred

under N<sub>2</sub> at room temperature for 20 hours. The resulting brown-red mixture was filtered using a glass wool filter pipet. The solvent was removed under reduced pressure to yield a dark brown solid. This dark brown solid was chromatographed using the same conditions as in the separation of Co(dc3). Upon adding dichloromethane, the light yellow band eluted first. The red band eluted second. A gray-black band could not be eluted. The solvent was removed from the two bands. The yellow solid was determined to be paramagnetic based on its NMR spectra.

## **2.3 Result and Discussion**

### **2.3.1 The Effect of KH on Co(dc3) Formation**

In his highest yield reaction, Chin et al.<sup>32</sup> was able to attain a yield of 24% for the synthesis of Co(dc3) using 2 equivalents of KH. Since then, we have not been able to obtain this high yield. However, as we increased the quantity of KH, we consistently obtained higher yield of Co(dc3) (Table 2.1). This piece of evidence lends support to our view that excess KH aids in the formation of Co(dc3), by deprotonation of the activated C-H bond.

Equivalents of KH	Co(dc3) yield
2.0	4.6 %
2.5	7.4 %
3.0	12 %
3.0 (step-wise addition)	10 %

**Table 2.1: The effect of using different equivalents of KH on the Co(dc3) yield.**

We also tried to separate the deprotonation of the ligand and the deprotonation of the agostic C-H bond by first adding two equivalents of KH to the H<sub>2</sub>dc<sub>3</sub> solution, and subsequently adding Co(acac)<sub>3</sub>, and stirring the solution for two hours. Then one more equivalent of KH was added. The yield for this step-wise addition experiment was similar to that of adding three equivalents at once.

### **2.3.2 NMR Experiments**

As mentioned above, the analysis of the <sup>1</sup>H and <sup>13</sup>C NMR spectra is difficult due to the low symmetry of the Co(dc<sub>3</sub>) complex. To completely analyze these two spectra, 2-D NMR experiments are necessary.

In 2-D experiments, due to the exchange of “information” between magnetic nuclei either through space or through bonds, a given nucleus may be encoded with information about the spin state of another nucleus. This encoding translates into coupling signals that are observable in a 2-D NMR spectrum. The strength of these couplings depend on whether the coupling is through space or through bond, the distance between the two magnetic nuclei and the angle between them

Two of the most frequently used 2-D NMR experiments are H-H Correlation Spectroscopy (COSY) and Heteronuclear Correlation Spectroscopy (HETCOR). In a COSY experiment, the chemical shift range of the proton spectrum is plotted on both the x & y axes. The coupling between protons can be observed as cross-peaks and information can be deduced from these couplings to give a complete analysis. Protons will couple best with themselves, thus strong couplings are observed on the diagonal axis. Couplings between geminal protons are the second strongest. The geminal coupling

constant is also dependent on the H-C-H angle,  $\alpha$ , and as a general rule, the geminal coupling constants increase as the angle  $\alpha$  decreases. Vicinal coupling constants are even weaker and they depend strongly on the dihedral angle,  $\beta$ , between the two protons. Generally, vicinal coupling constant is at maximum when the dihedral angle is at  $0^\circ$ , at minimum when the dihedral angle is at  $90^\circ$ , and at maximum when the dihedral angle is at  $180^\circ$ .

In a HETCOR experiment, the chemical shift range of the proton spectrum is plotted on one axis while the chemical shift range of the  $^{13}\text{C}$  NMR spectrum for the same sample is plotted on the second axis. In this experiment, strong one-bond coupling is observed. The parameters are typically optimized so that two and three-bond couplings are not observed. The COSY and HETCOR data appears in Appendix 2

To completely analyze the  $^1\text{H}$  and  $^{13}\text{C}$  NMR spectra, we utilized a complementary approach between COSY and HETCOR to assign the NMR spectra. In the  $^{13}\text{C}$  NMR spectrum, there are three signals that can be assigned:  $\delta$  -10.53 ppm: C-8,  $\delta$  176.69 ppm: C-2,  $\delta$  25.13 ppm: C-6. The assignment of C-8 is based on the fact that carbons bound to  $\text{Co}^{\text{III}}$  are typically shifted upfield of 0 ppm.<sup>37</sup> In the  $^1\text{H}$  NMR spectrum, we could not definitively assign any signal.

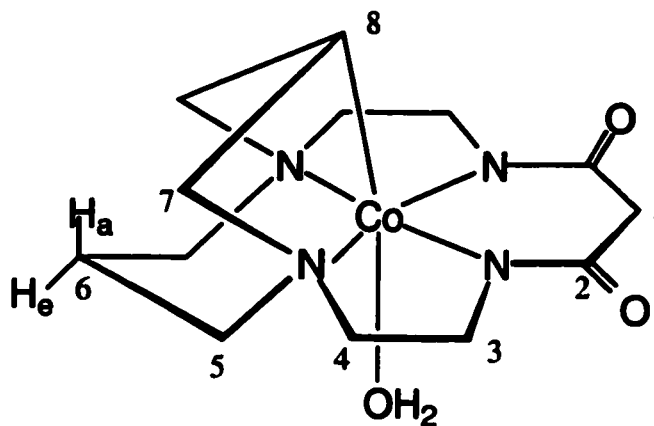


**Figure 2.1:** Co(dc3).

In the HETCOR, we observe that C-8 couples with a proton signal ( $\delta$  2.12 ppm), thus, this signal is assigned H-8. In the COSY, we observe that H-8 couples with a multiplet ( $\delta$  3.80 ppm). This multiplet is assigned to a proton on C-7. Other protons are at least three bonds away. In COSY, this proton signal is also strongly coupled with another proton signal ( $\delta$  3.2 ppm, multiplet). Due to the nature of the carbon strap, the two protons attached to C-7 are exposed to different chemical environment. These two protons thus appear at different chemical shifts ( $\delta$  3.80 ppm and  $\delta$  3.20 ppm). Since we are able to assign the protons on C-7 from COSY, using the HETCOR, we can also assign C-7 ( $\delta$  64.79 ppm). The HETCOR also bolsters the previous assignment that there are two different protons on C-7. Since we know C-6 from its chemical shift, we can use HETCOR to determine the protons attached to C-6. C-6 couples to protons at  $\delta$  2.02 (broad doublet) and  $\delta$  2.64 (multiplet). From crystal structure, the carbon strap containing C-6 has a locked chair conformation, thus one proton on C-6 is in an

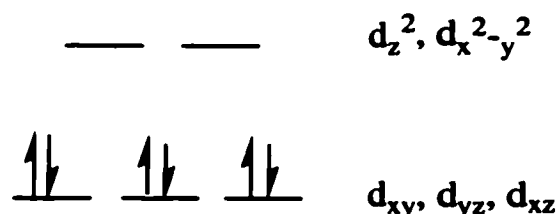
equatorial position ( $H_e$ ) and the other proton is in an axial position ( $H_a$ ). In this case, the differentiation between  $H_a$  and  $H_e$  can be achieved.  $H-6_a$  is assigned to  $\delta$  2.64 (multiplet) because it couples strongly to the vicinal axial protons on two C-5s and to  $H-6_e$ .  $H-6_e$  however, only couples strongly with  $H-6_a$ ; thus its signal appears as a doublet at  $\delta$  2.02. The broadening of the  $H-6_e$  signal is due to the weak coupling between  $H-6_e$  and the vicinal equatorial protons on C-5. Now that the protons on C-6 are known, the protons on C-5 can be determined using COSY. These signals show up at  $\delta$  2.50 (doublet) and  $\delta$  2.75 ppm (multiplet). Again, two protons attached to the same carbon have different chemical shifts. The C-5 resonance is then assigned using the HETCOR. In the  $^{13}\text{C}$  NMR spectrum, the only three signals not assigned yet are  $\delta$  61.07 ppm,  $\delta$  45.92 ppm, and  $\delta$  45.67 ppm. Among those,  $\delta$  45.92 ppm has the smallest peak size (less than half the size of the other two signals). In addition, the three carbons remaining (C-1, C-3, and C-4) are all directly attached to 2 protons, thus are Nuclear Overhauser-enhanced by a similar ratio. Since there is only one C-1, two C-3s, and two C-4s, C-1 is assigned to  $\delta$  45.92 ppm. From the HETCOR, we can assign the protons attached to C-1 ( $H-1$ ,  $\delta$  3.32 ppm). The only two remaining signals in the  $^{13}\text{C}$  NMR spectrum are  $\delta$  61.07 ppm and  $\delta$  45.67 ppm. These two signals corresponded to C-3 and C-4. Since C-3 is bonded to an amide nitrogen and C-4 is bonded to an amine nitrogen, C-3 should be more downfield. C-3 is therefore assigned at  $\delta$  61.07 ppm and C-4 is assigned at  $\delta$  45.67 ppm. Now that we are able to completely assign the  $^{13}\text{C}$  NMR spectrum, we can use HETCOR to determine the protons that are attached to C-3 and C-4. The protons that are attached to

C-3 are assigned at  $\delta$  2.75 ppm (multiplet) and  $\delta$  2.64 ppm (multiplet). The protons that are attached to C-4 are assigned at  $\delta$  3.20 ppm and  $\delta$  3.60 ppm (multiplet).

### 2.3.3 Electrochemistry of Co(dc3)

As stated previously, we would like to break the Co-C bond and to reform the C-H bond, so that we can subsequently try to monitor C-H bond activation. The addition of triflic acid was not successful due to the strength of the Co-C bond. Perhaps an electrochemical method for this bond cleavage might prove useful.

The electron diagram for Co(dc3) can be drawn as shown in Figure 2.2.



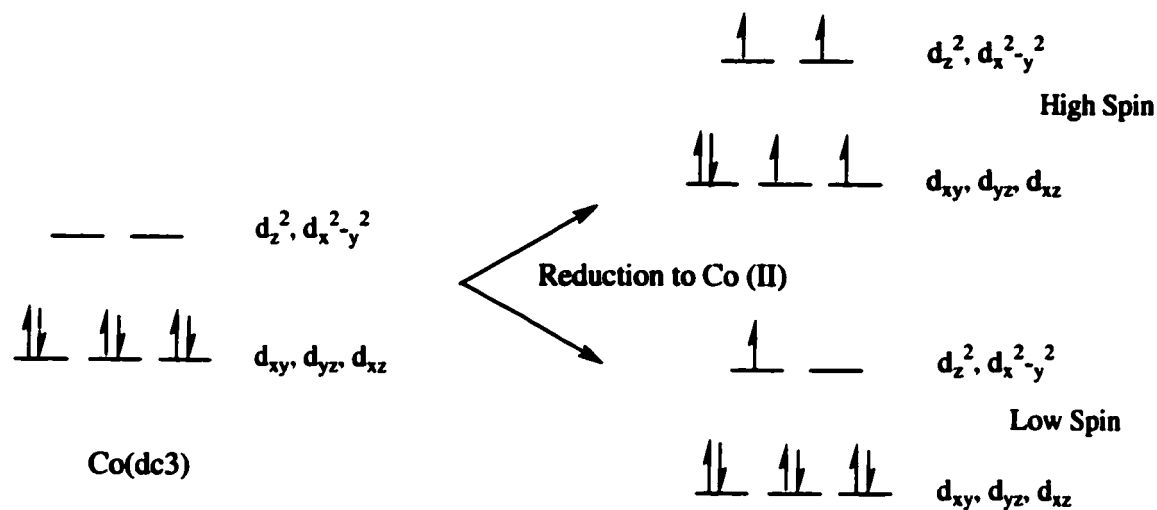
Co(dc3)

Figure 2.2: Electron diagram of Co(dc3).

In an octahedral field, the d orbitals of the cobalt metal are split into two bands,  $t_{2g}$  and  $e_g$ . In the  $e_g$  band, there are  $d_z^2$  and  $d_x^2-y^2$  orbitals. Within the  $t_{2g}$  band, there are  $d_{xy}$ ,  $d_{yz}$ , and  $d_{xz}$  orbitals. Since Co(dc3) is diamagnetic, its six d electrons are all arranged in the  $t_{2g}$  band.

Upon reduction to  $\text{Co}^{\text{II}}$ , the complex can either be low spin or high spin.

Regardless of whether the  $\text{Co}^{\text{II}}(\text{dc}3)$  is high spin or low spin, it will have electron density in the  $d_z^2$  orbital (Figure 2.3).



**Figure 2.3:** Possible electron diagrams of  $\text{Co}^{\text{II}}$  complex.

Because the  $d_z^2$  orbital is the recipient of two electrons from the  $sp^3$  orbital of carbon in the Co-C bond, any electron input into the  $d_z^2$  orbital will create electron-electron repulsion. This repulsion could lead to the rupture of the Co-C bond (Figure 2.4).

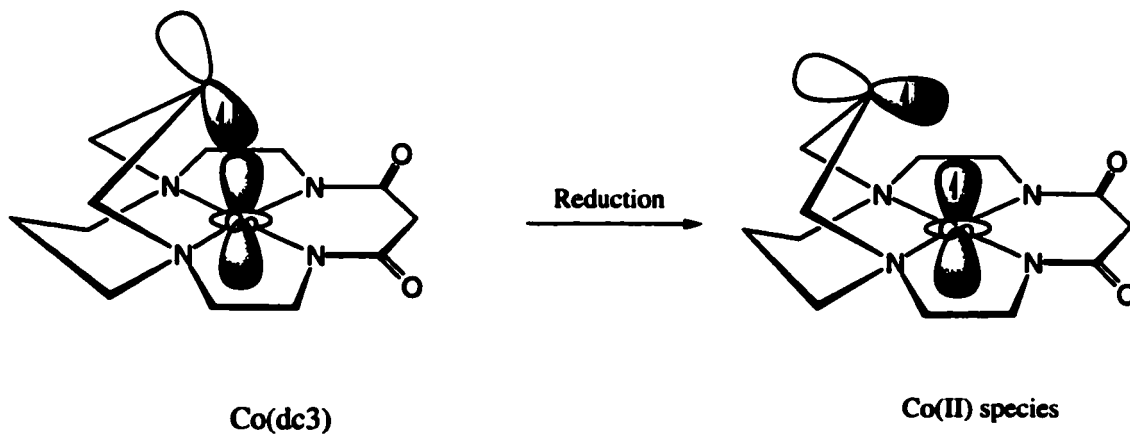


**Figure 2.4:** The rupture of the Co-C bond.



To determine if reduction will indeed lead to rupture of the cobalt-carbon bond, we have investigated the electrochemistry using cyclic voltammetry. The initial potential was set to 0 V vs. Ag/AgCl and was chosen because that is a resting potential for the complex (no electrolysis will occur when the electrode is switched on). The initial scan is toward negative potential. At  $\sim -0.8$  V, the potential is sufficiently negative to reduce  $\text{Co}^{\text{III}}(\text{dc}3)$  and a cathodic current was observed. The cathodic current increases rapidly and levels out at  $\sim -1.0$  V. The current then decays. Upon scanning back toward positive potentials, no return wave was observed (Figure 2.5).

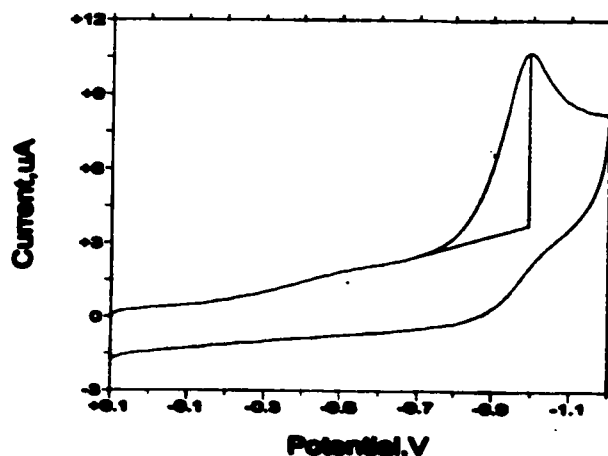


**Figure 2.5:** Cyclic voltammogram of  $\text{Co}(\text{dc}3)$ .

The absence of a return wave indicates that a chemical step has occurred following electron transfer. The likely explanation is that the Co-C bond has been ruptured by the reduction from  $\text{Co}^{\text{III}}$  to  $\text{Co}^{\text{II}}$  and that the new complex has a different oxidation potential.

This observation is similar to the reduction of vitamin B<sub>12</sub>. In vitamin B<sub>12</sub>, the reduction of Co<sup>III</sup> to Co<sup>II</sup> also leads to the cleavage of a Co-C bond.<sup>38</sup> (Figure 2.6)

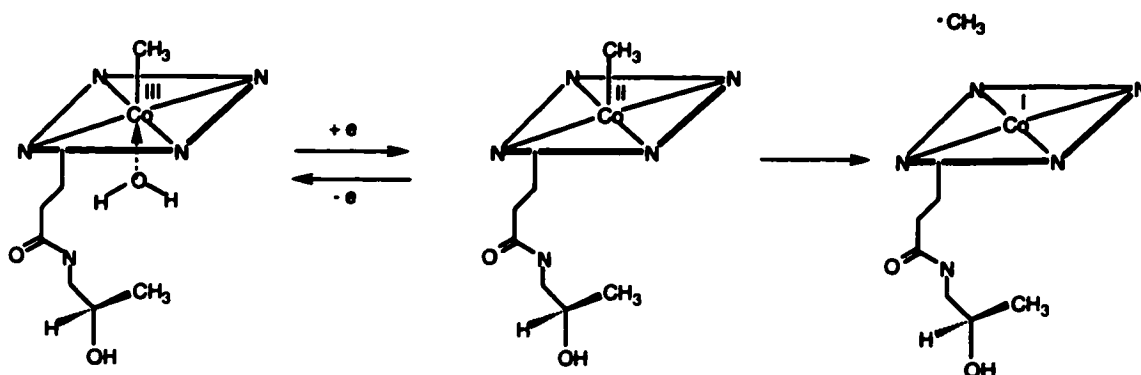


**Figure 2.6:** The rupture of a Co-C bond in Cobalamin by reduction of Co<sup>III</sup> to Co<sup>II</sup>.

Another similar aspect of the electrochemistry of Co(dc3) and Cobalamin is in the reduction potential. In vitamin B<sub>12</sub>, the Co<sup>III/II</sup> reduction potential occurs in the range of -1.0 V to -1.6 V vs. Standard Hydrogen Electrode.<sup>38</sup> For the above cobalamin which resemble Codc3 the most (having water and an alkyl as axial ligands), the reduction potential is -1.46 V vs. Standard Calomel Electrode.<sup>38</sup> The breaking of Co-C bond in Co(dc3) by reduction demonstrates that we may be able to perform this step chemically. In addition, the results of this study suggest that Co(dc3) can be used as a model compound for studying the properties of vitamin B<sub>12</sub>.

### **2.3.4 Attempts to Chemically Reduce Co(dc3) by Bis(cyclopentadienyl)cobalt**

The previous experiment suggests that the cobalt-carbon bond in Co(dc3) can be cleaved by the electrochemical reduction of the cobalt center. We were interested in finding whether this could be done preparatively by the addition of a chemical reducing agent. Upon addition of bis(cyclopentadienyl)cobalt to Co(dc3), a color change was

observed. Chromatographic separation yielded a yellow solid. Because of the paramagnetic properties of this yellow species, the signals in the  $^1\text{H}$  and  $^{13}\text{C}$  NMR spectra are extremely broad such that useful information about the compound structure could not be deduced. The possibility that the yellow solid is the product of the reaction between bis(cyclopentadienyl)cobalt and dichloromethane was ruled out based on the result of a control reaction between bis(cyclopentadienyl)cobalt and dichloromethane. The yellow species is also not cobalticinium because cobalticinium, despite having a yellow color, is diamagnetic.<sup>39</sup> The remaining possibility is that the yellow species is  $\text{Co}^{\text{II}}(\text{dc}3)$ . Unfortunately, time constraints did not allow us to elucidate further the identity of this yellow species.

**Chapter 3: Synthesis and Characterization of a New  
Constrained Tetraazamacrocyclic, Its Metallation and  
Protonation Reactions**

### 3.1 Introduction

The Co(dc3) system demonstrated that this ligand type promotes cleavage of the C-H bond, likely due to an electrophilic C-H bond activation mode. However, due to the necessary chemical conditions required to metallate H<sub>2</sub>dc3 (the addition of a base), we were unable to observe the Co-H-C intermediate of the activation process

Because one of our goals is to observe intermediates on the path to C-H bond activation, we devised another strapped cyclam ligand that does not require the addition of a base for the metallation reaction. This new ligand is 1,11-C<sub>3</sub>-cyclam which is prepared from H<sub>2</sub>dc3 as shown in Figure 3.1.



**Figure 3.1:** The preparation of 1,11-C<sub>3</sub>-cyclam from H<sub>2</sub>dc3.

Due to the structural similarity of H<sub>2</sub>dc3 and 1,11-C<sub>3</sub>-cyclam, we believe that this new ligand should also impose an interaction between the C-H bond of the ligand and the coordinated metal.

Although sharing the same architecture as the H<sub>2</sub>dc3 ligand, 1,11-C<sub>3</sub>-cyclam differs significantly in its role as a ligand. 1,11-C<sub>3</sub>-cyclam is not deprotonated upon metallation and is therefore a neutral ligand, whereas, H<sub>2</sub>dc3 needs to be deprotonated at

both amide nitrogens making it a 2- ligand. This charge difference will likely have a profound impact on the chemistry of the corresponding metal complex.

## **3.2 Experimental**

### **3.2.1 Materials and Methods**

Borane-tetrahydrofuran complex (1.0 M) was purchased and used as received. Elemental analyses of 1,11-C<sub>3</sub>-cyclam were obtained from Atlantic Microlab, Norcross, GA. Silica gel 60 (230-400 mesh ASTM, particle size 0.040-0.063 mm) was purchased and used as received. All other materials were purchased and used as received. pH measurements were recorded on an Orion pH meter model 710A, that was standardized with pH 10 and pH 12 buffers. The water used in this pH experiment was HPLC grade and was boiled prior to use. Conductivity experiments were performed using a Fisher Scientific conductivity apparatus Model AB30.

### **3.2.2 Synthesis of 1,11-C<sub>3</sub>-cyclam**

H<sub>2</sub>dc3 (622 mg, 2.317 mmol) was placed into a 3-neck round bottom flask fitted with a water condenser, a glass stopper, and a rubber septum. The system was purged with N<sub>2</sub> gas. BH<sub>3</sub>·THF (1M, 15 mL) was added using a syringe. The heterogeneous mixture was stirred under N<sub>2</sub> gas at room temperature for 5 minutes, the septum was replaced with a glass stopper, and the mixture was refluxed for 72 hours under N<sub>2</sub> gas. Dry MeOH (3 mL) was then added drop-wise to the cooled mixture to quench the excess borane. After the effervescence ceased, HCl (3M, 5mL) was added drop-wise and the solution was stirred for ten minutes. Evaporation of the organic solvent was performed using rotary evaporation. MeOH (10 mL) was added to the residue. The solvent was

removed again. Repetition of the previous step (addition of MeOH and evaporation) was performed three more times to aid the removal of the trimethyl borate (which forms a low-boiling azeotrope with methanol). In the last evaporation, the solution was evaporated to dryness. To the residue, 3M HCl (14 mL) was added to dissolve the white solid. Dichloromethane (13mL) was added subsequently, and the organic layer was discarded. Aqueous KOH solution (15M, 10mL) was added to the aqueous solution drop-wise. After the effervescence ceased, the product was extracted with 5×30 mL of dichloromethane. Evaporation of dichloromethane to dryness yielded a crude oily product (373mg, yield 67%). Purification of the crude product was performed by vacuum sublimation (45°C, 50 millitorr). Pure 1,11-C<sub>3</sub>-cyclam was removed from the cold finger in the dry box. Yield 278 mg (50%). <sup>1</sup>H NMR data: CDCl<sub>3</sub>, 21°C, δ 2.62 (t, 4H), δ 2.52 (m, 12H), δ 2.48 (t, 4H), δ 1.54 (quintet, 2H), δ 1.62 (m, 2H), δ 1.42 (m, 2H). <sup>13</sup>C NMR data: CDCl<sub>3</sub>, 21°C, δ 57.96, δ 53.87, δ 47.95, δ 46.38, δ 30.70, δ 28.73. Anal. Calc. C<sub>13</sub>H<sub>28</sub>N<sub>4</sub>: C, 34.01; H, 5.71; N, 14.16 . Found: C, 34.09; H, 5.68; N, 14.26.

### **3.2.3 Attempts to Synthesize [Co(1,11-C<sub>3</sub>-cyclam)(NO<sub>2</sub>)<sub>2</sub>]ClO<sub>4</sub>**

To a round bottom flask containing 60 mL H<sub>2</sub>O was added Na<sub>3</sub>[Co(NO<sub>2</sub>)<sub>6</sub>] (0.550 g, 1.36 mmol). To a round bottom flask containing 21 mL H<sub>2</sub>O was added 1,11-C<sub>3</sub>-cyclam (0.300 g, 1.25 mmol). The two solutions were mixed together and the resulting solution was warmed on an oil bath at 78°C for 35 minutes. Upon cooling, the solution was filtered to give a bright orange solution. NaClO<sub>4</sub> (10 g) was added to the stirred solution. The solution was left overnight in a refrigerator (5°C). Faint yellow crystals precipitated out of the solution and were collected and recrystallized from water to yield

colorless crystals of  $[\text{H}_2\text{1,11-C}_3\text{-cyclam}](\text{ClO}_4)_2$ .  $^1\text{H}$  NMR and  $^{13}\text{C}$  NMR spectra are in Appendix 3.  $^1\text{H}$  NMR data:  $\text{CD}_3\text{CN}$ ,  $21^\circ\text{C}$ ,  $\delta$  3.14 (m, 12H),  $\delta$  3.00 (m, 4H),  $\delta$  2.92 (m, 4H),  $\delta$  2.14 (m, 2H),  $\delta$  1.86 (m, 2H),  $\delta$  1.76 (m, 2H).  $^{13}\text{C}$  NMR data:  $\text{CD}_3\text{CN}$ ,  $21^\circ\text{C}$ ,  $\delta$  57.27,  $\delta$  55.04,  $\delta$  51.03,  $\delta$  46.18,  $\delta$  25.68,  $\delta$  24.81. Anal. Calc  $\text{C}_{13}\text{H}_{30}\text{N}_4\text{Cl}_2\text{O}_8$ : C, 35.38; H, 6.85; N, 12.69. Found: C, 35.87; H, 6.65; N, 12.72.

### **3.2.4 Synthesis of $[\text{Co}(\text{1,11-C}_3\text{-cyclam})(\text{NCS})_2]\text{SCN}$**

In a dry box, 1,11- $\text{C}_3$ -cyclam (150 mg, 0.624mmol) was added to a round bottom flask equipped with a stir bar and containing 25 mL of dry acetonitrile. The solution was stirred to dissolve the ligand. Subsequently, NaSCN (190 mg, 2.340 mmol) and  $\text{CoCl}_2$  (103 mg, 0.800 mmol) were added to the solution. The solution turned yellow-green. The flask was then attached to a water condenser, capped, and brought out of the dry box. The mixture was stirred and refluxed under a  $\text{N}_2$  gas blanket for one day. The solution showed a deep green color. The mixture was cooled to room temperature, charcoal (500 mg) was added and air was bubbled into the mixture for another day during which the color changed to dark blue. The blue mixture was filtered and the solvent was removed under reduced pressure. The product was separated by column chromatography (Silica gel,  $1\text{cm}\times 20\text{cm}$ , 20:80 mixture of  $\text{MeOH}:\text{CH}_2\text{Cl}_2$ ). The pink band was collected and the solvent was removed under reduced pressure to yield  $[\text{Co}(\text{1,11-C}_3\text{-cyclam})(\text{NCS})_2]\text{SCN}$  (54 mg, 18%).  $^1\text{H}$  NMR and  $^{13}\text{C}$  NMR spectra are shown in Appendix 3.  $^1\text{H}$  NMR data:  $\text{CD}_3\text{OD}$ ,  $21^\circ\text{C}$ ,  $\delta$  3.45 (m),  $\delta$  3.32 (s),  $\delta$  2.95 (m),  $\delta$  2.65 (m),  $\delta$  2.52 (m),  $\delta$  2.1 (m),  $\delta$  1.75 (m).  $^{13}\text{C}$  NMR data:  $\text{CD}_3\text{OD}$ ,  $21^\circ\text{C}$ ,  $\delta$  65.01,  $\delta$  61.96,  $\delta$  57.38,  $\delta$  53.26,  $\delta$  49.48,  $\delta$  28.59,  $\delta$  26.09,  $\delta$  25.10.



### 3.3 Results and Discussion

#### 3.3.1 1,11-C<sub>3</sub>-cyclam Synthesis and Reactivity

In theory, the synthesis of 1,11-C<sub>3</sub>-cyclam could be done by either attaching a three-carbon long strap to cyclam or by reducing H<sub>2</sub>dc3 (Figure 3.2).

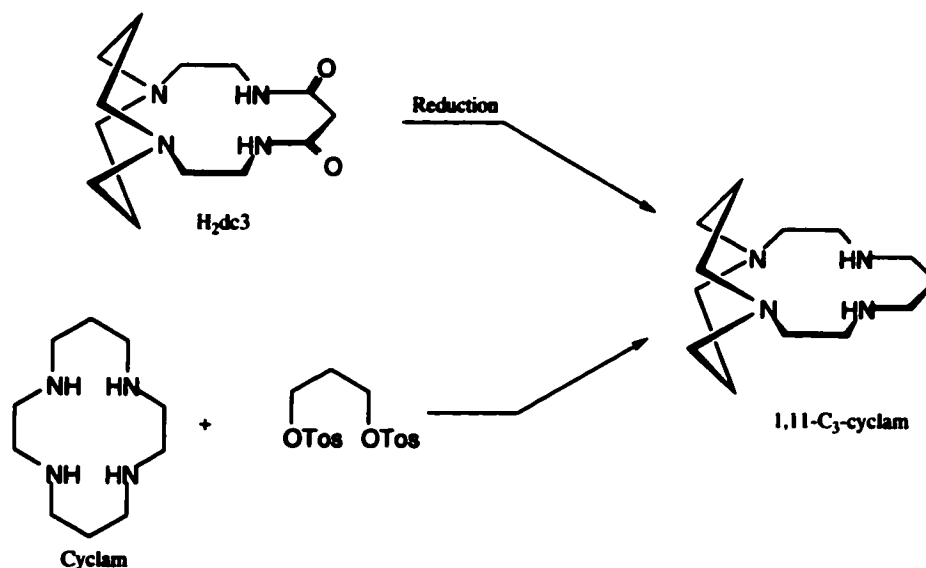


**Figure 3.2:** Possible routes for the synthesis of 1,11-C<sub>3</sub>-cyclam.

Although the attachment of a three-carbon long strap to cyclam seems to be a more simple approach because cyclam is commercially available and synthetic procedures for adding a strap to macrocyclic polyaza compounds are known,<sup>36,40,41</sup> the synthesis of 1,11-C<sub>3</sub>-cyclam by this route could potentially give byproducts (Figure 3.3), resulting in a lengthy purification.

To avoid this isolation step, we utilized the already characterized H<sub>2</sub>dc3 as the starting material. The reduction of cyclic amides using borane is well known and often gives high yield.<sup>42</sup> We therefore opted for this synthetic scheme.

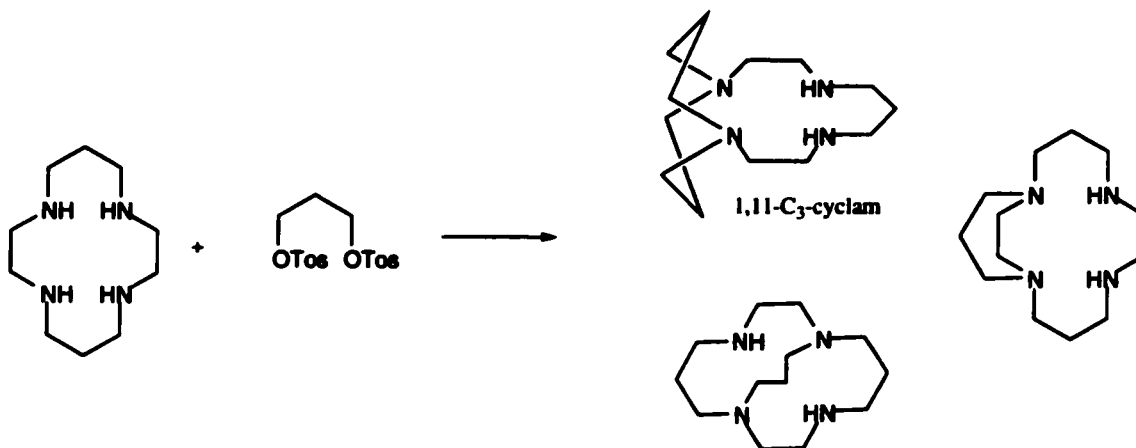


**Figure 3.3:** Possible byproducts for the bridging alkylation of cyclam.

After refluxing  $\text{H}_2\text{dc3}$  in 1M  $\text{BH}_3/\text{THF}$  solution for three days, dry methanol was added to the cooled solution to react with excess borane to form a trimethyl borate complex and hydrogen gas. This trimethyl borate complex was subsequently evaporated under reduced pressure. Aqueous HCl was added to make sure that all amines were fully protonated. The protonated compound is very polar and can be extracted easily from methylene chloride by water. The aqueous solution was then treated with concentrated aqueous KOH to deprotonate the previously protonated amine. Once deprotonated, the compound is relatively non-polar and can be extracted from water by methylene chloride.

Both the  $^1\text{H}$  and  $^{13}\text{C}$  NMR spectra of 1,11- $\text{C}_3$ -cyclam (Appendix 3) show two separate groups of signals, one downfield and one upfield. The downfield group of signals in the  $^1\text{H}$  NMR spectrum corresponds to the protons on the carbons in the  $\alpha$  position to an amine while the upfield group corresponds to the protons on the carbons in the  $\beta$  position to an amine (Figure 3.4). There is a vertical internal mirror plane bisecting

the molecule into two equivalent parts. There is also a horizontal internal mirror plane. As a result, the two three-carbon straps are identical and the front side of the molecule is identical to the back side of the molecule. The geometry of the molecule causes the two protons on C-5 to be chemically inequivalent and have different chemical shifts; the same is true of the protons on C-6. Inequivalent protons on the same carbon should be strongly coupled.

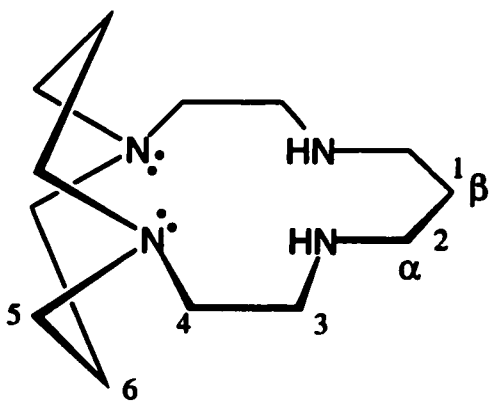


**Figure 3.4:** 1,11-C<sub>3</sub>-cyclam.

The multiplet  $\delta$  1.41 is assigned to one proton attached to C-6 and the other multiplet at  $\delta$  1.61 is assigned to the other proton attached to C-6. The protons on C-1 are assigned to be the quintet at  $\delta$  1.74. The identity of the triplet at  $\delta$  2.61, a triplet at  $\delta$  2.49 and a multiplet at  $\delta$  2.52 is hard to ascertain. However, based on the similarity in chemical environments, we propose a tentative assignment. The triplet at  $\delta$  2.61 and triplet at  $\delta$  2.49 correspond to protons attached to either C-3 or C-4. The multiplet at  $\delta$  2.52 (12H) corresponds to all the protons on C-5 and C-2. Integration of the number of protons strongly supports our assignment of 1,11-C<sub>3</sub>-cyclam. Using the same logic, we

tentatively assign the  $^{13}\text{C}$  NMR spectrum as follows:  $\delta$  28.73 (C-1),  $\delta$  30.70 (C-6),  $\delta$  46.38 and  $\delta$  47.94 (C-3 and C-4),  $\delta$  53.84 (C-5), and  $\delta$  57.96 (C-2). Having obtained the desired ligand, we now wish to insert cobalt into the ligand.

Poon's metallation procedure for cyclam was initially adopted for the attempted synthesis of  $[\text{Co}(1,11\text{-C}_3\text{-cyclam})(\text{NO}_2)_2]\text{ClO}_4$ .<sup>43</sup> Using this procedure for the metallation of 1,11- $\text{C}_3$ -cyclam, white crystals were obtained. Both  $^{13}\text{C}$  and  $^1\text{H}$  NMR spectra of the product show ligand characteristics, but the NMR spectra are different from the NMR spectra of the ligand. Additionally, being a white crystal, the product does not fit the profile of inorganic complexes. To further determine whether the resulting compound is our proposed product, we tested the conductivity of this compound. In acetonitrile, a  $1.00 \times 10^{-3}\text{M}$  solution of the product has a conductivity of 254  $\mu\text{S}$ . From the conductivity, the molar conductance ( $\Lambda\text{m}$ ) was found to be  $273 \Omega^{-1}\text{mol}^{-1}\text{cm}^{-1}$ . In acetonitrile, this value of molar conductance corresponds to three ions, inconsistent with our desired product (2 ions). Elemental analysis suggested that the product is  $[\text{H}_2 1,11\text{-C}_3\text{-cyclam}](\text{ClO}_4)_2$ , the salt of the diprotonated ligand (Figure 3.5).

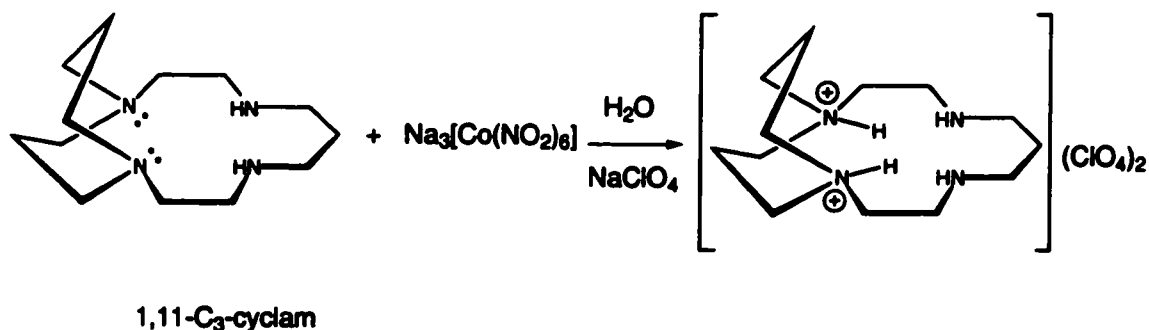


**Figure 3.5:** Formation of  $[\text{H}_2 1,11\text{-C}_3\text{-cyclam}](\text{ClO}_4)_2$ .

In a separate experiment, 1,11-C<sub>3</sub>-cyclam was allowed to react with less than one equivalent of aqueous HCl. The product of this reaction was determined to be diprotonated ligand based on conductivity experiments and <sup>1</sup>H NMR spectroscopy. The formation of diprotonated ligand instead of monoprotonated ligand, even when there is less than one equivalent of HCl suggests that water can also protonate this ligand.

Given that the product of the metallation of 1,11-C<sub>3</sub>-cyclam in water is [H<sub>2</sub> 1,11-C<sub>3</sub>-cyclam](ClO<sub>4</sub>)<sub>2</sub> and 1,11-C<sub>3</sub>-cyclam appears to deprotonate water, how can we rationalize the formation of this protonated species instead of the desired [Co(1,11-C<sub>3</sub>-cyclam)(NO<sub>2</sub>)<sub>2</sub>]ClO<sub>4</sub>, when this procedure works for cyclam? What factors inhibit the metallation of 1,11-C<sub>3</sub>-cyclam? Our result suggests that the protonation of 1,11-C<sub>3</sub>-cyclam may inhibit the metallation process by making the lone pairs unavailable to bind to the metal. If this is the case, then why does this problem occur only in the metallation of 1,11-C<sub>3</sub>-cyclam and not in the metallation of cyclam?

Looking more closely into the difference between the structure of cyclam and 1,11-C<sub>3</sub>-cyclam, a small but significant difference is revealed. Two of the secondary amines in cyclam have been converted to two tertiary amines in 1,11-C<sub>3</sub>-cyclam. Besides being tertiary amines, the extra constraint resulting from the steric repulsion within the 1,5 diazacyclooctane subunit of 1,11-C<sub>3</sub>-cyclam renders these nitrogens relatively fixed in space. This causes the two lone pairs on the amine nitrogens to point toward one focal point. Thus, a proton could feel the attraction of both lone pairs. Normally, lone pairs resist positioning in close proximity to each other due to electron repulsion. However, in this ligand, the electron repulsion from the straps is substantially higher than that of two

lone pairs in close proximity. As a result, the compound adopts this locked orientation of lone pairs.

This behavior of 1,11-C<sub>3</sub>-cyclam is similar to the behavior of the well-known proton sponge (Figure 3.6). In proton sponge, due to steric repulsion, the two methyl groups from one amine are directed away from the two methyl group of the adjacent amine. As a result, the two lone electron pairs are pointed toward the same middle point. The position of two lone electron pairs in this way increases significantly the basicity of this class of amines, thus the term proton sponge.

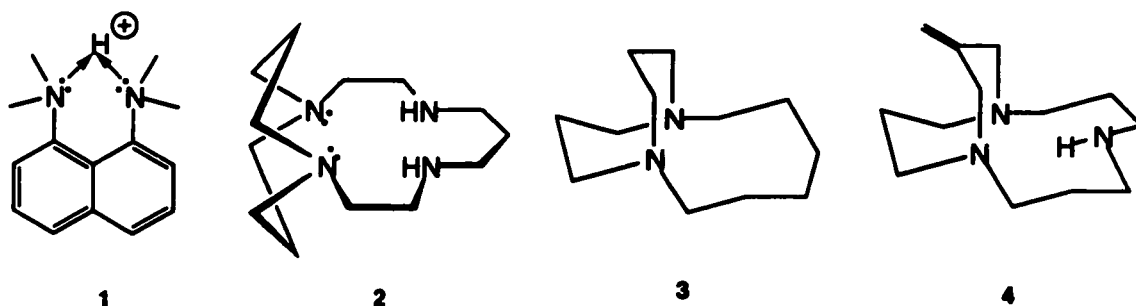


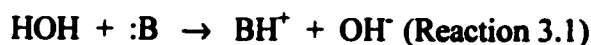
**Figure 3.6:** Structure of proton sponge (1), 1,11-C<sub>3</sub>-cyclam (2), 1,8-diazabicyclo[6.3.3]tetradecane(3), and 11-methylene-1,5,9-triazabicyclo[7.3.3.]pentadecane(4).

Other compounds containing the 1,5-diazacyclooctane (daco) subunit like 1,11-C<sub>3</sub>-cyclam that display “proton sponge”-like character are 3 and 4 (Figure 3.6). Alder et al.<sup>44,45</sup> showed that the internally protonated species of 3 is very stable, but it forms extremely slowly (prolonged heating in acid) because the protonation site is shielded. Bell et al.<sup>41</sup> showed that the incorporation of a basic site (amine) in the macrocycle provides a pathway for protonation, thus resulting in the immediate formation of

internally protonated species of 4. In 1,11-C<sub>3</sub>-cyclam, two secondary amines provide a pathway for rapid protonation.

To quantify the basicity of 1,11-C<sub>3</sub>-cyclam, we need to determine the pK<sub>a</sub> of the protonated form of the ligand. Previous experiments indicated that 1,11-C<sub>3</sub>-cyclam can deprotonate water; thus pH measurement can be used to find pK<sub>a</sub> of the protonated form of 1,11-C<sub>3</sub>-cyclam.

Let us consider the reaction between a base and water.



By measuring the pH, one can determine [OH<sup>-</sup>]<sub>eq</sub>. From [OH<sup>-</sup>]<sub>eq</sub>, [BH<sup>+</sup>]<sub>eq</sub> can be deduced. Applying the equations shown below, the pK<sub>a</sub> of the monoprotonated ligand can be found.

$$K_{\text{eq}} = \frac{[\text{BH}^+][\text{OH}^-]}{[\text{HOH}][\text{:B}]} \rightleftharpoons \frac{[\text{HOH}]}{[\text{:B}]} K_{\text{eq}} = \frac{[\text{OH}^-][\text{BH}^+]}{[\text{:B}]}$$

$$\rightleftharpoons K_{\text{b}} = \frac{[\text{OH}^-][\text{BH}^+]}{[\text{:B}]}$$

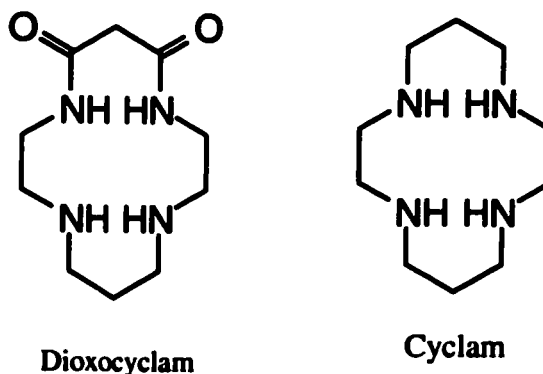
$$K_{\text{a}} K_{\text{b}} = K_{\text{w}}$$

Using this conversion, we were able to determine the pK<sub>a</sub> value of the conjugate acid of the ligand (Table 3.1).

<u>Amines</u>	<u>Concentration</u>	<u>pH</u>	<u>pK<sub>a</sub></u>
H <sub>2</sub> dc3	0.018 M	11.95	12.1
1,11-C <sub>3</sub> -cyclam	0.034 M	12.50	≥ 13.5

**Table 3.1:  $pK_a$  of protonated amines.**

Compared to the  $pK_a$  of protonated cyclam ( $pK_a = 11.50$ ),<sup>46</sup> the  $pK_a$  of protonated 1,11- $C_3$ -cyclam is at least 2.0 units higher. The  $pK_a$  for protonated  $H_2dc3$  is approximately 2.4 units higher than the  $pK_a$  of protonated dioxocyclam ( $pK_a = 9.67$ ).<sup>46</sup>



This similar  $pK_a$  increases for  $H_2dc3$  relative to dioxocyclam and for 1,11- $C_3$ -cyclam relative to cyclam suggests that the increases in  $pK_a$  is likely due to the constrained nature of the two straps as described previously. This result is not surprising considering that the  $pK_a$  of the protonated form of **4** is  $>13.5$ .<sup>41</sup>

### **3.3.2 Synthesis of [Co(1,11- $C_3$ -cyclam)(NCS)<sub>2</sub>]SCN**

The difficulty of metallation of 1,11- $C_3$ -cyclam in protic solvents suggests the necessity of using aprotic anhydrous solvents. The solvent of choice is dry acetonitrile. In addition, a stepwise approach was chosen, that is, metallation using the labile  $Co^{II}$ , followed by air-oxidation to the substitutionally inert  $Co^{III}$ .

TLC demonstrates that the mixture consists of three colored components: pink, faint green, and red. This observation also suggests that silica gel can also be used to



separate the charged species. Upon elution, the pink band eluted first followed by the red band. The faint green band could not be eluted.

Although NMR signals of the red species appear to have the same chemical shifts as that of the pink species, the broadness of the NMR signals in the red species' spectrum indicates that the red species has more paramagnetic character than the pink species has.

The identification of the product is carried out by NMR spectroscopy and X-ray crystallography. In the  $^{13}\text{C}$  NMR spectrum, the pink component shows eight peaks. This suggests that the two carbon straps on the ligand are not equivalent. One possible reason is that two N-H protons are on the same side of the  $\text{N}_4$  plane. Hu <sup>47</sup> was able to synthesize  $[\text{Co}(1,11\text{-C}_3\text{-cyclam})(\text{NCS})_2]\text{OTf}$ . Since  $[\text{Co}(1,11\text{-C}_3\text{-cyclam})(\text{NCS})_2]\text{SCN}$  and  $[\text{Co}(1,11\text{-C}_3\text{-cyclam})(\text{NCS})_2]\text{OTf}$  have the same  $^1\text{H}$  and  $^{13}\text{C}$  NMR spectra, information obtained for  $[\text{Co}(1,11\text{-C}_3\text{-cyclam})(\text{NCS})_2]\text{OTf}$  can be applied to  $[\text{Co}(1,11\text{-C}_3\text{-cyclam})(\text{NCS})_2]\text{SCN}$ . The crystal structure of  $[\text{Co}(1,11\text{-C}_3\text{-cyclam})(\text{NCS})_2]\text{OTf}$  (Appendix 3) is in agreement with the assigned positions of two N-H protons.

### **3.4 Conclusion**

Although the metallation of 1,11- $\text{C}_3$ -cyclam has been achieved, the resulting complex does not exhibit the interaction between the C-H bond of one carbon strap and the metal. Rather, the two axial sites are occupied by two linear isothiocyanate groups. Hu <sup>47</sup> suggests that the size of the axial ligand in the  $[\text{Co}(1,11\text{-C}_3\text{-cyclam})(\text{NCS})_2]\text{OTf}$  complex is not bulky enough to exert steric repulsion onto the carbon straps. As a result, the carbon straps are not forced to interact with the metal. This leaves a vacant site for

**another isothiocyanate ligand to approach the metal. In the future, Hu et al. will attempt to use bulkier ligands to prove this hypothesis.**

## References

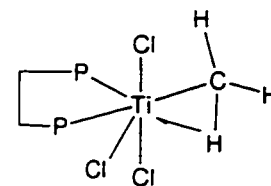
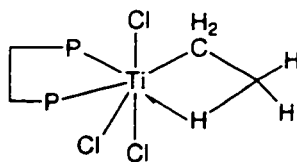
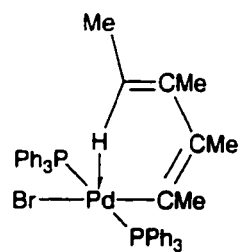
1. Data from National Petrochemical and Refiners Association.
2. McMurry J.; *Organic Chemistry*, 2<sup>nd</sup> ed.; Brooks/Cole: Pacific Grove, California, 1988; Chapter 5, p141.
3. Crabtree, R.H. *Chem. Rev.* **1985**, *85*, 245.
4. Sono, M.; Roach, M.P.; Coulter, E.D.; Dawson, J.H. *Chem. Rev.* **1996**, *96*, 2841.
5. Davydov, R.; Makris, T.M.; Kofman, V.; Werst, D.E.; Sligar, S.G.; Hoffman, B.M. *J. Am. Soc. Chem.* **2001**, *123*, 1403.
6. Groves, J.T.; McClusky, G.A. *J. Am. Chem. Soc.* **1976**, *98*, 859.
7. Toy, P.H.; Newcomb, M.; Hollenberg, P.F. *J. Am. Chem. Soc.* **1998**, *120*, 7719.
8. Hjelmeland, L.M.; Aronow, L.; Trudell, J.R. *Biochem. Biophys. Res. Commun.* **1977**, *76*, 541.
9. Newcomb, M.; Shen, R.; Choi, S.; Toy, P.H.; Hollenberg, P.F.; Vaz, A.D.; Coon, M.J. *J. Am. Chem. Soc.* **2000**, *122*, 2677.
10. Collman, J.P.; Chien, A.S.; Eberspacher, T.A.; Brauman, J.I. *J. Am. Chem. Soc.* **1998**, *120*, 425.
11. Wallar, B.J.; Lipscomb, J.D. *Chem. Rev.* **1996**, *96*, 2625.
12. Rosenzweig, A.C.; Frederick, C.A.; Lippard, S.J.; Nordlund, P. *Nature* **1993**, *366*, 537.
13. (a) Stetter, H. and Goebel, P. *Chem. Ber.* **1962**, *95*, 1040; (b) Olah, G.A. *Top. Curr. Chem.* **1980**, *80*, 17.
14. Davis, S.C.; Klabunde, K.J. *J. Am. Chem. Soc.* **1978**, *100*, 5973.
15. Barrett, P.H.; Pasternak, M.; Pearson, R.G. *J. Am. Chem. Soc.* **1979**, *101*, 222.
16. Muller, J. and Goll, J. *Chem. Ber.* **1973**, *106*, 1129.

17. Halle, L.F.; Houriet, R.; Staley, R.H.; Beauchamp, J.L. *J. Am. Chem. Soc.* **1982**, *104*, 6293.
18. Halle, L.F.; Armentrout, P.B.; Beauchamp, J.L. *Organometallics* **1982**, *1*, 963.
19. a) Fokin, A.A.; Schreiner, P.R. *Chem. Rev.* **2002**, *102*, 1551; b) Mayer, J.M. *Acc. Chem. Res.* **1998**, *31*, 441.
20. a) Muetterties, E.L. *Centenary Lecture on Hydrocarbon Reactions at Metal Centres*, RSC Dalton Division Meeting, London, 1982; b) Bengali, A.A.; Schultz, R.H.; Moor, C.; Bergman, R.G. *J. Am. Chem. Soc.* **1994**, *116*, 9585; c) Haddleton, D.M.; McCamley, A.; Perutz, R.N. *J. Am. Chem. Soc.* **1988**, *110*, 1810; d) Periana, R.A.; Bergman, R.G. *J. Am. Chem. Soc.* **1986**, *108*, 7332.
21. Broderick, W.E.; Kanamori, K.; Willett, R.D.; Legg, J.I. *Inorg. Chem.* **1991**, *30*, 3875.
22. Crabtree, R.H.; Lavin, M. *J. Chem. Soc., Chem. Commun.* **1985**, 794.
23. Brookhart, M. and Green, M.L. *J. Organomet. Chem.* **1983**, *250*, 395.
24. Chatt, J. and Davidson, J.M. *J. Chem. Soc.* **1965**, 843.
25. Parshall, G.W. *Acc. Chem. Res.* **1970**, *3*, 139.
26. Janowicz, A.H. and Bergman, R.G. *J. Am. Chem. Soc.* **1982**, *104*, 352.
27. Janowicz, A.H. and Bergman, R.G. *J. Am. Chem. Soc.* **1983**, *105*, 3929.
28. Jones, W.D. and Feher, F.J. *J. Am. Chem. Soc.* **1982**, *104*, 4240.
29. Hoyano, J.K. and Graham, W.A.G. *J. Am. Chem. Soc.* **1982**, *104*, 3722.
30. Lian, T.; Bromberg, S.E.; Yang, H.; Proulx, G.; Bergman, R.G.; Harris, C.B. *J. Am. Chem. Soc.* **1996**, *118*, 3769.
31. Geftakis, S.; Ball, G.E. *J. Am. Chem. Soc.* **1998**, *120*, 9953.
32. Chin, M.; Nguyen, K.; Wagenknecht, P.S. unpublished results.
33. Lexa, D. and Saveant, J. *Acc. Chem. Res.* **1983**, *16*, 235.
34. Kim, M. and Birke, R. *J. Electroanal. Chem.* **1983**, *144*, 331.

35. Huang, Q. and Gosser, D.K. *Talanta* **1992**, 39(9), 1155.
36. Chin, M.; Wone, D.; Nguyen, Q.; Nathan, L.C.; Wagenknecht, P.S. *Inorg. Chim. Acta* **1999**, 292, 254.
37. Buckingham, A.D. and Stephens, P.J. *J. Chem. Soc.* **1964**, 2747.
38. Krautler, B. *B<sub>12</sub> Electrochemistry and Organometallic Electrochemical Synthesis*, Innsbruck, Austria, **1999**, p315.
39. Schmid, G; Hoehner, U.; Kampmann, D.; Zaika, D.; Boese, R. *J. Organomet. Chem.* **1983**, 256(2), 225.
40. Wainwright, K.P. *Inorg. Chem.* **1980**, 19, 1396.
41. Bell, T.W.; Choi, H.; Harte, W. *J. Am. Chem. Soc.* **1986**, 108, 7427.
42. Parker, D. *Macrocyclic Synthesis*, Oxford University Press, Oxford, London, **1996**, p26.
43. Mok, K.S. and Poon, C.K. *Inorg. Chem.* **1971**, 10, 225.
44. Alder, R.W.; Sessions, R.B. *Tetrahedron Lett.* **1982**, 23, 1121.
45. Alder, R.W.; Moss, R.E.; Sessions, R.B. *J. Chem. Soc., Chem. Commun.* **1983**, 997-998.
46. Zhu, S.; Kou, F.; Lin, H.; Lin, C.; Lin, M.; Chen, Y. *Inorg. Chem.* **1996**, 35, 5851.
47. Hu, C.; Nguyen, T.; Lawrence, N.; Wagenknecht, P.S. manuscript is submitted for publication.

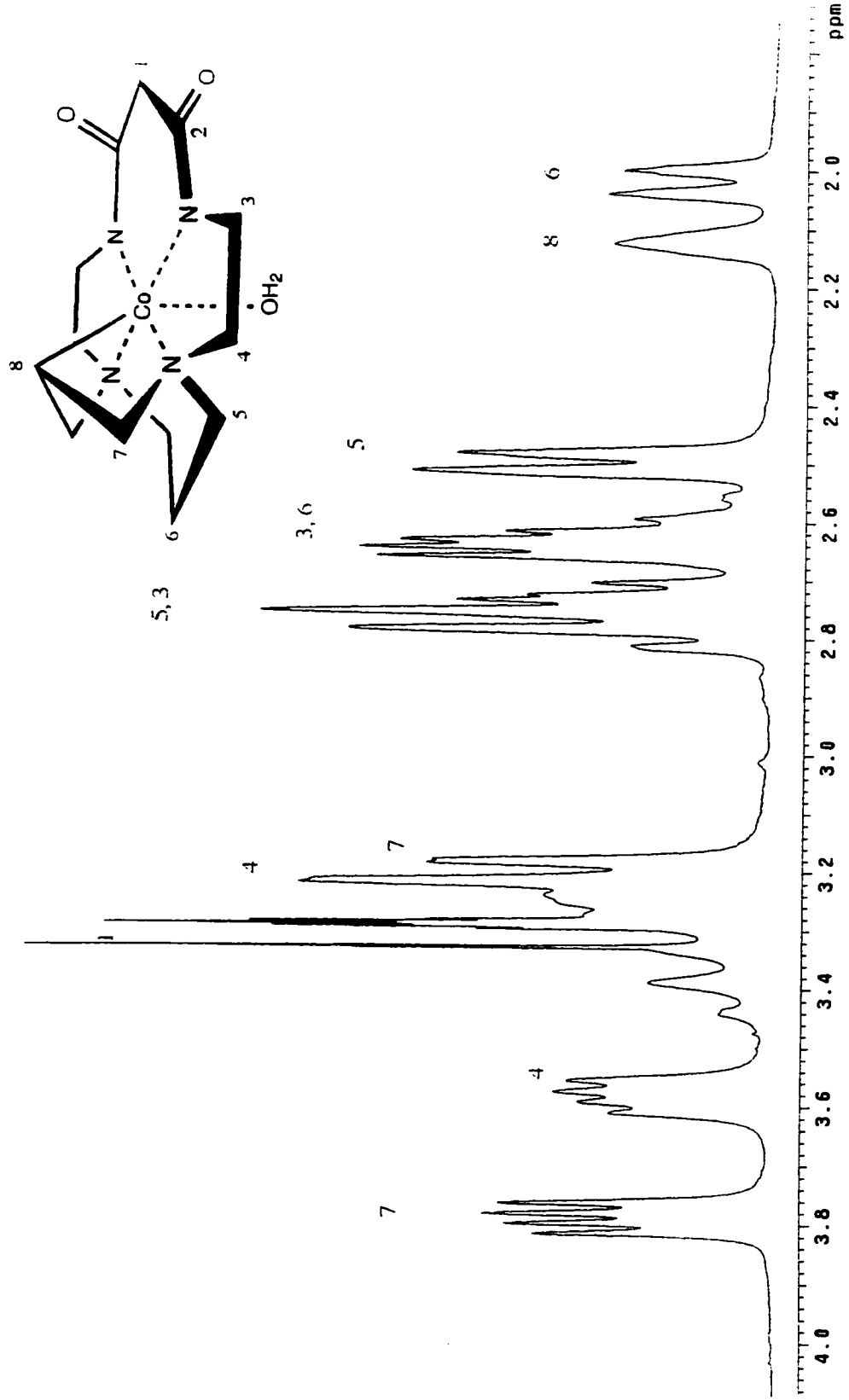
## **Appendix 1**

### **Additional Figures and NMR Spectra for Chapter 1**



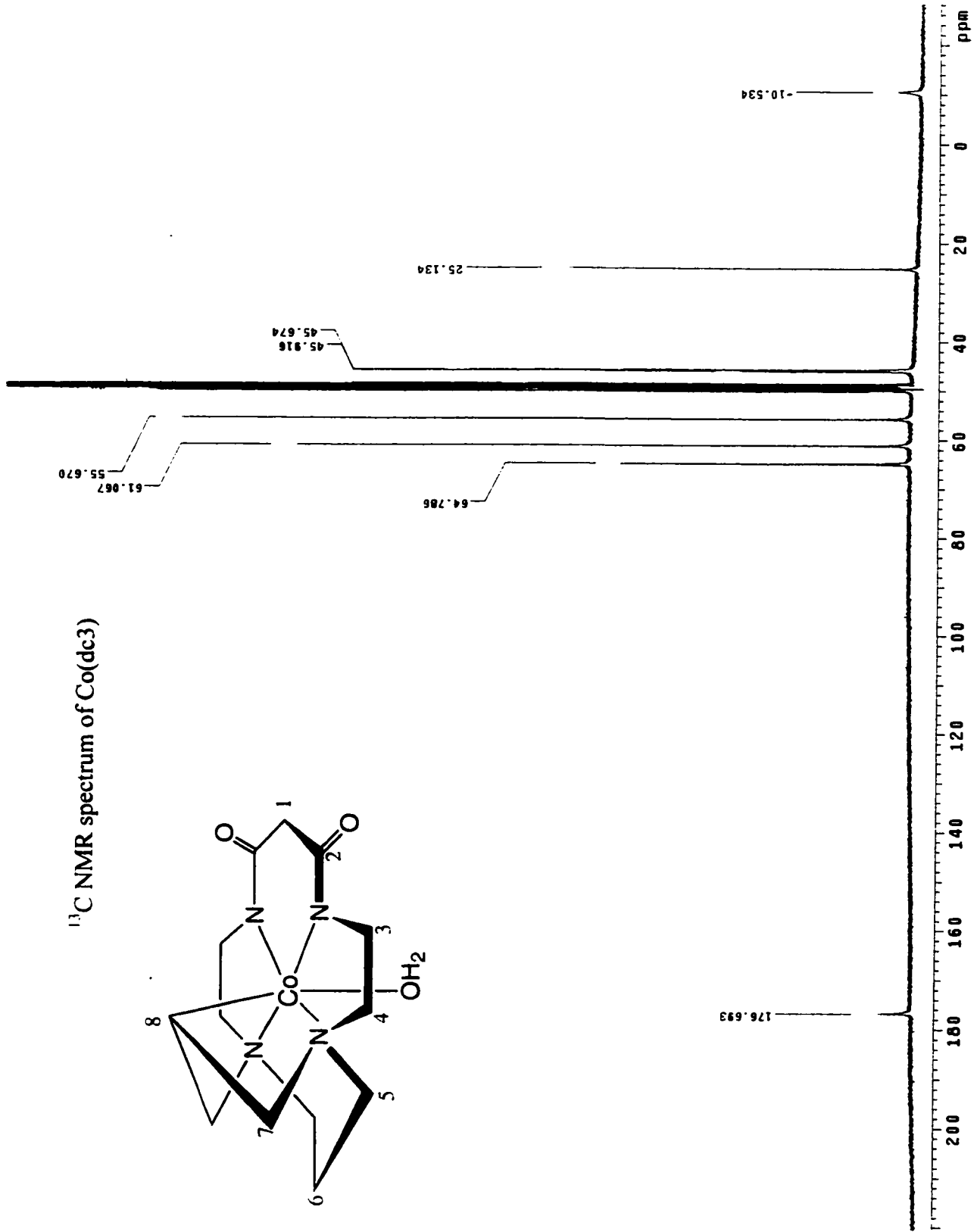
Examples of C-H-M interaction (taken from ref 3)

$^1\text{H}$  NMR spectrum of  $\text{Co}(\text{dc3})$

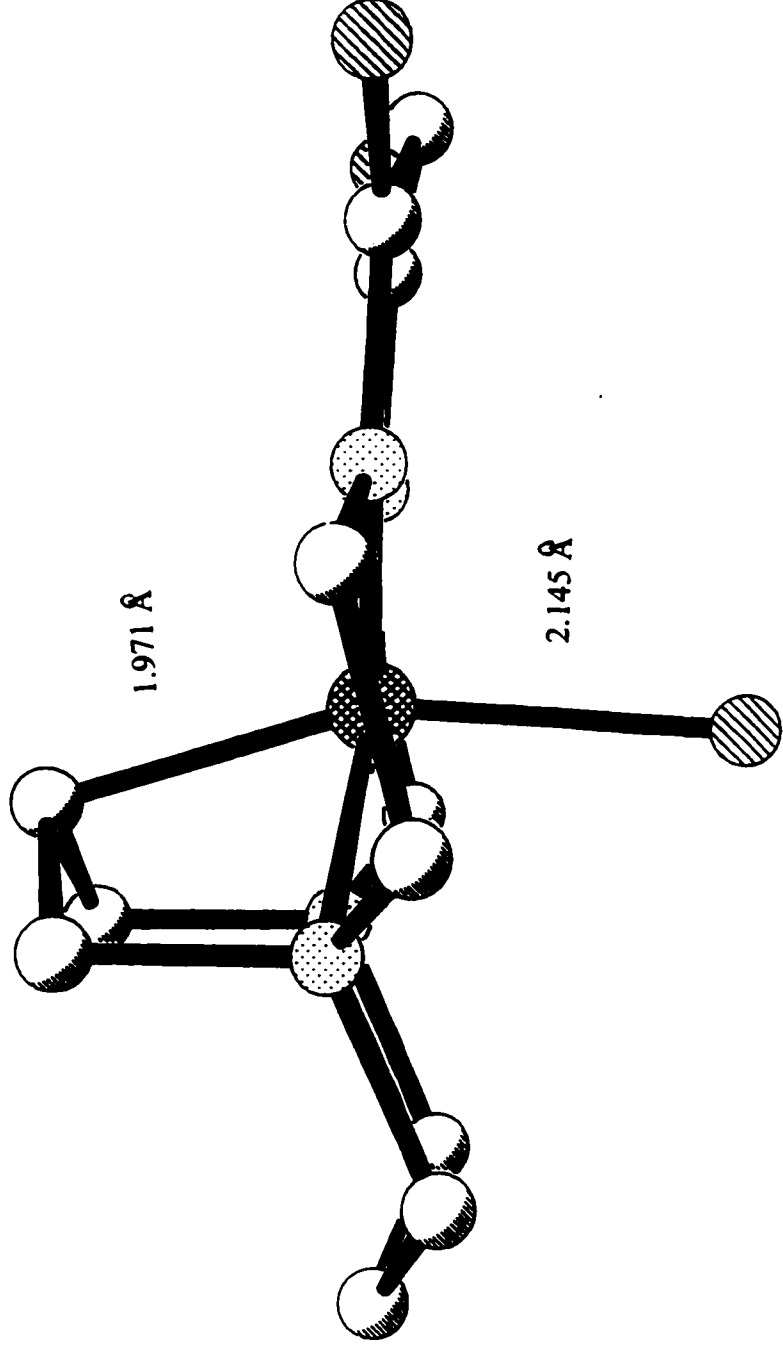




$^{13}\text{C}$  NMR spectrum of  $\text{Co}(\text{dc3})$



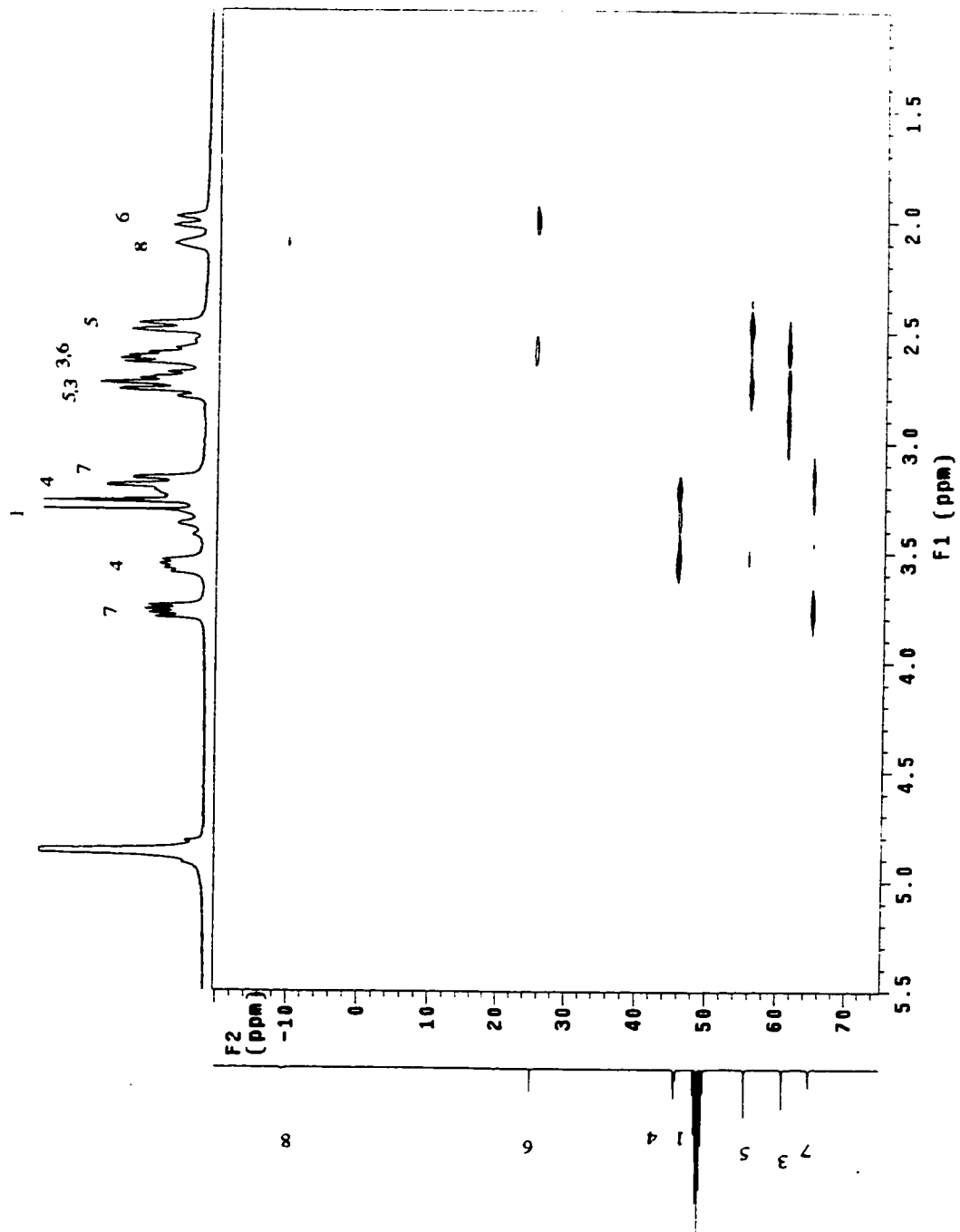
Crystal structure of  $\text{Co}(\text{dc3})\text{H}_2\text{O}$



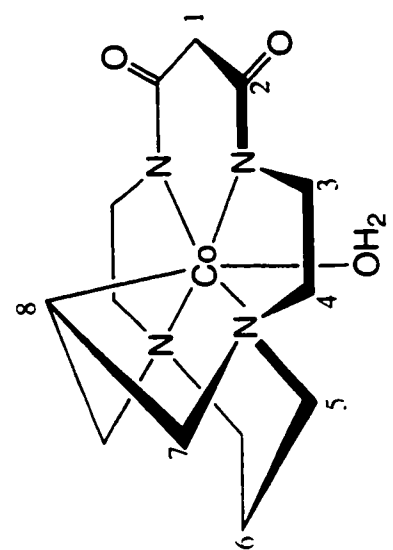
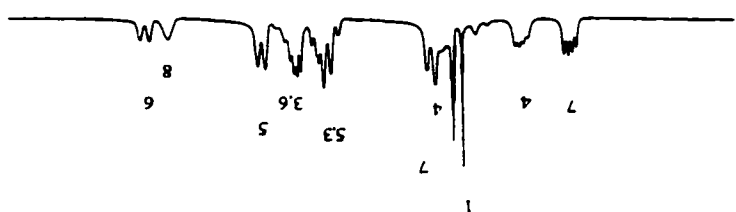
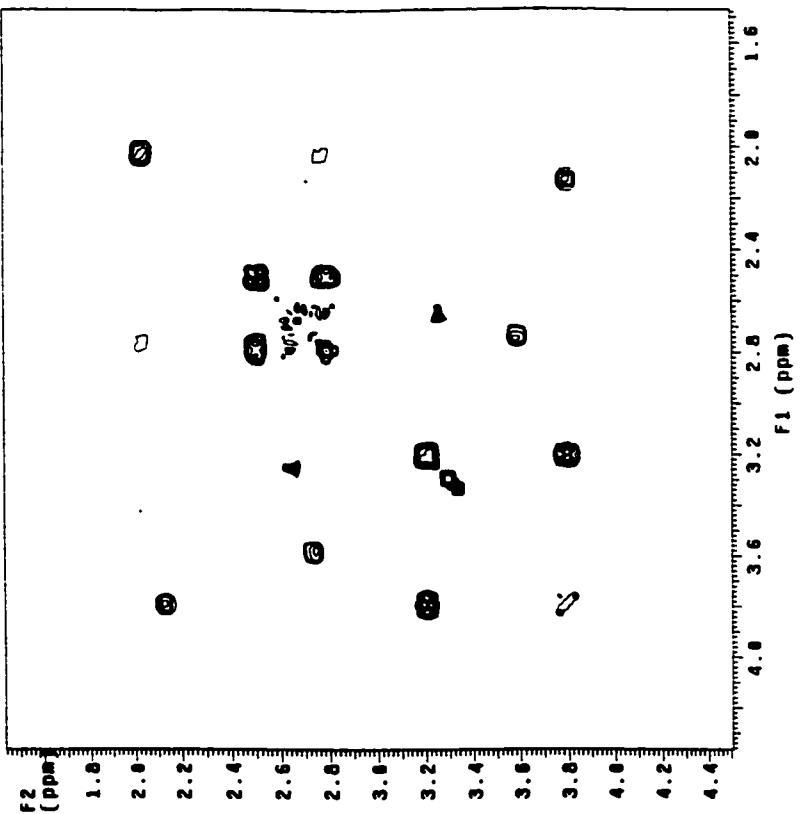
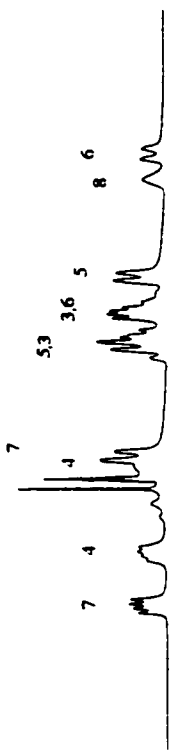
Performed by Prof. Lawrence Nathan, SCU

**Appendix 2**  
**Additional NMR Spectra for Chapter 2**

HETCOR spectrum of Co(dc3)



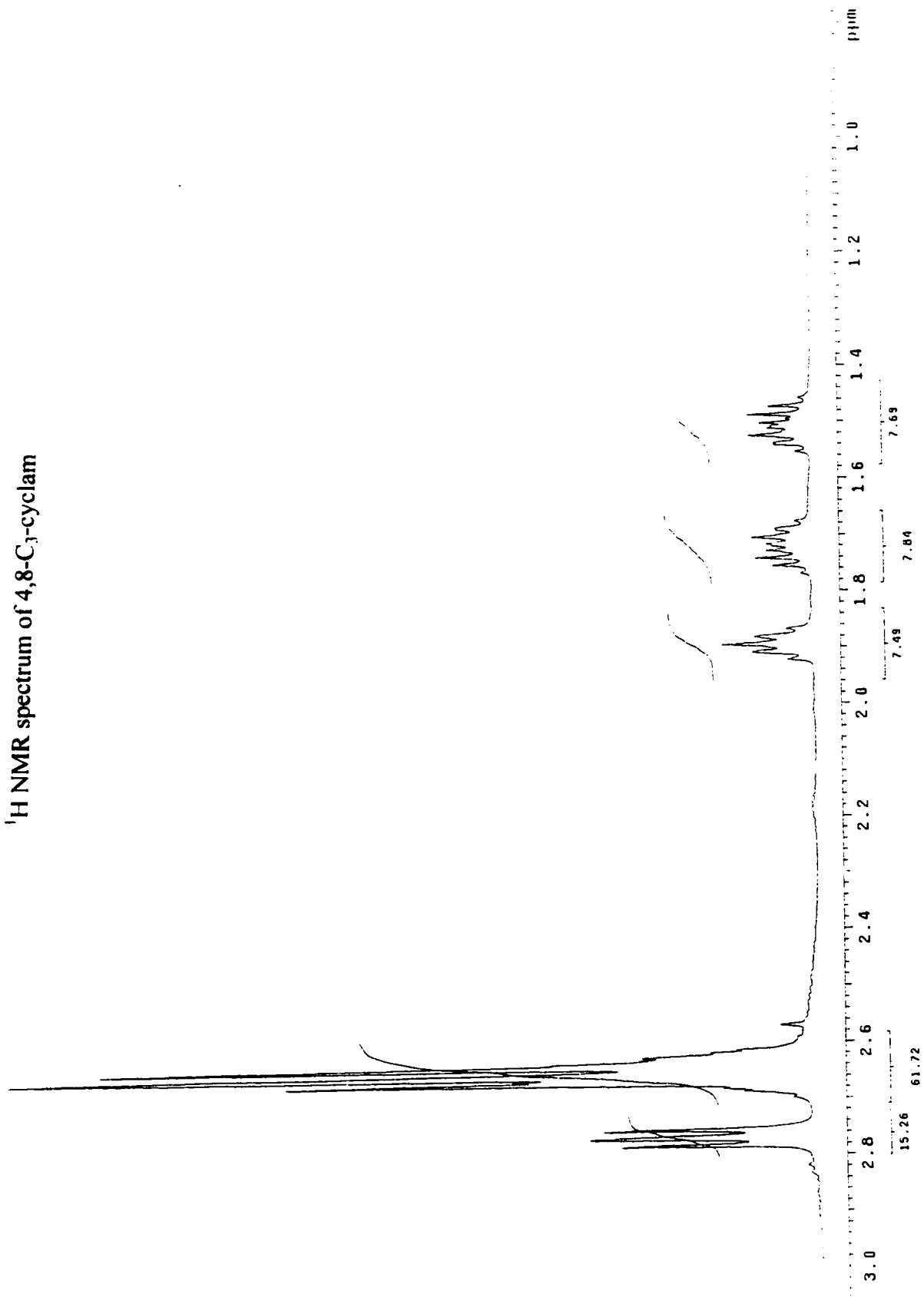
CCSY spectrum of Co(dc3)



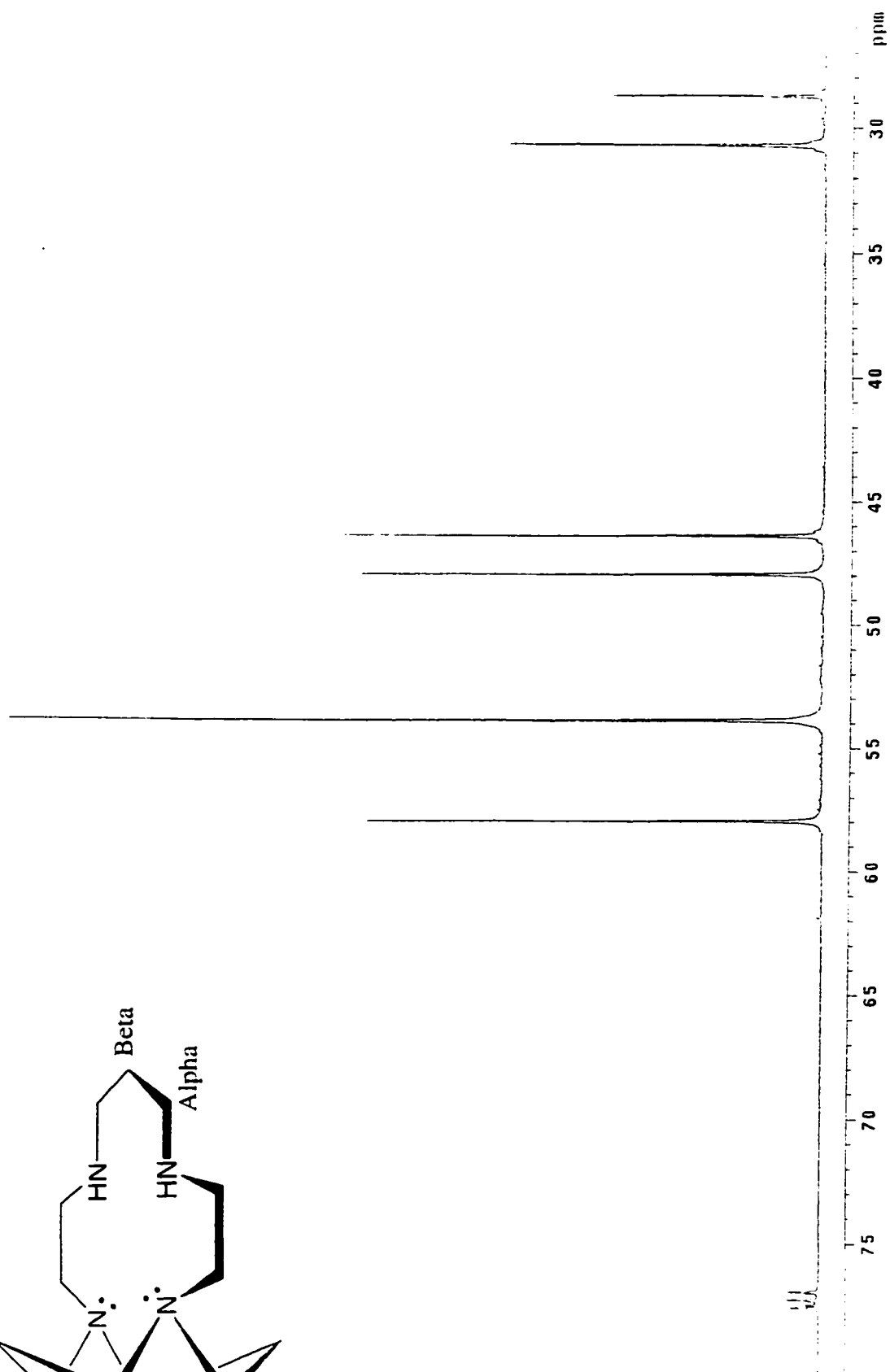
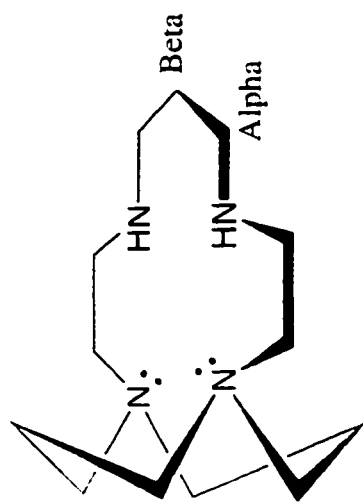
## **Appendix 3**

### **Additional Figure and NMR spectra for Chapter 3**

<sup>1</sup>H NMR spectrum of 4,8-C<sub>3</sub>-cyclam

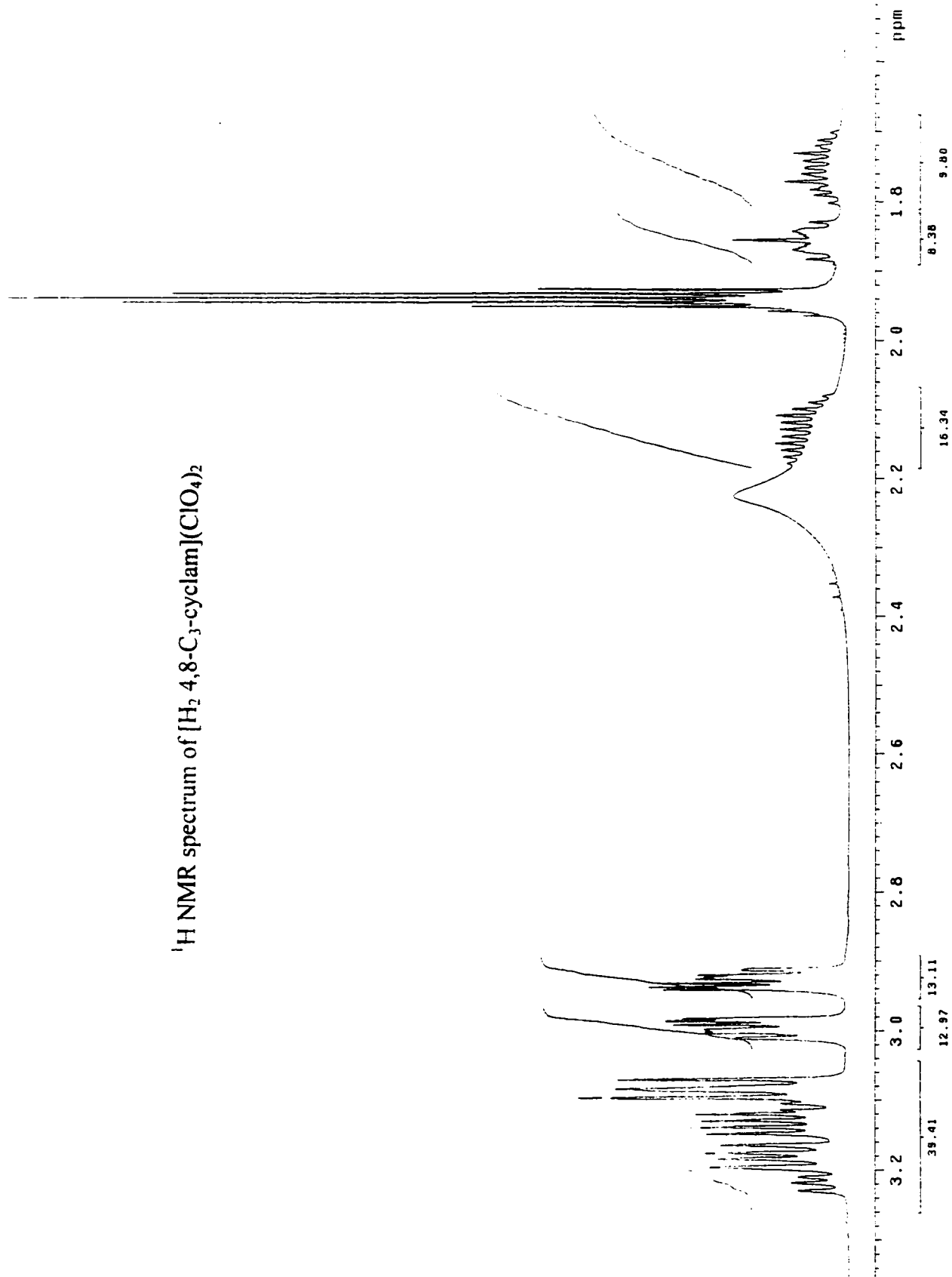


$^{13}\text{C}$  NMR spectrum of 4,8- $\text{C}_3\text{-cyclam}$

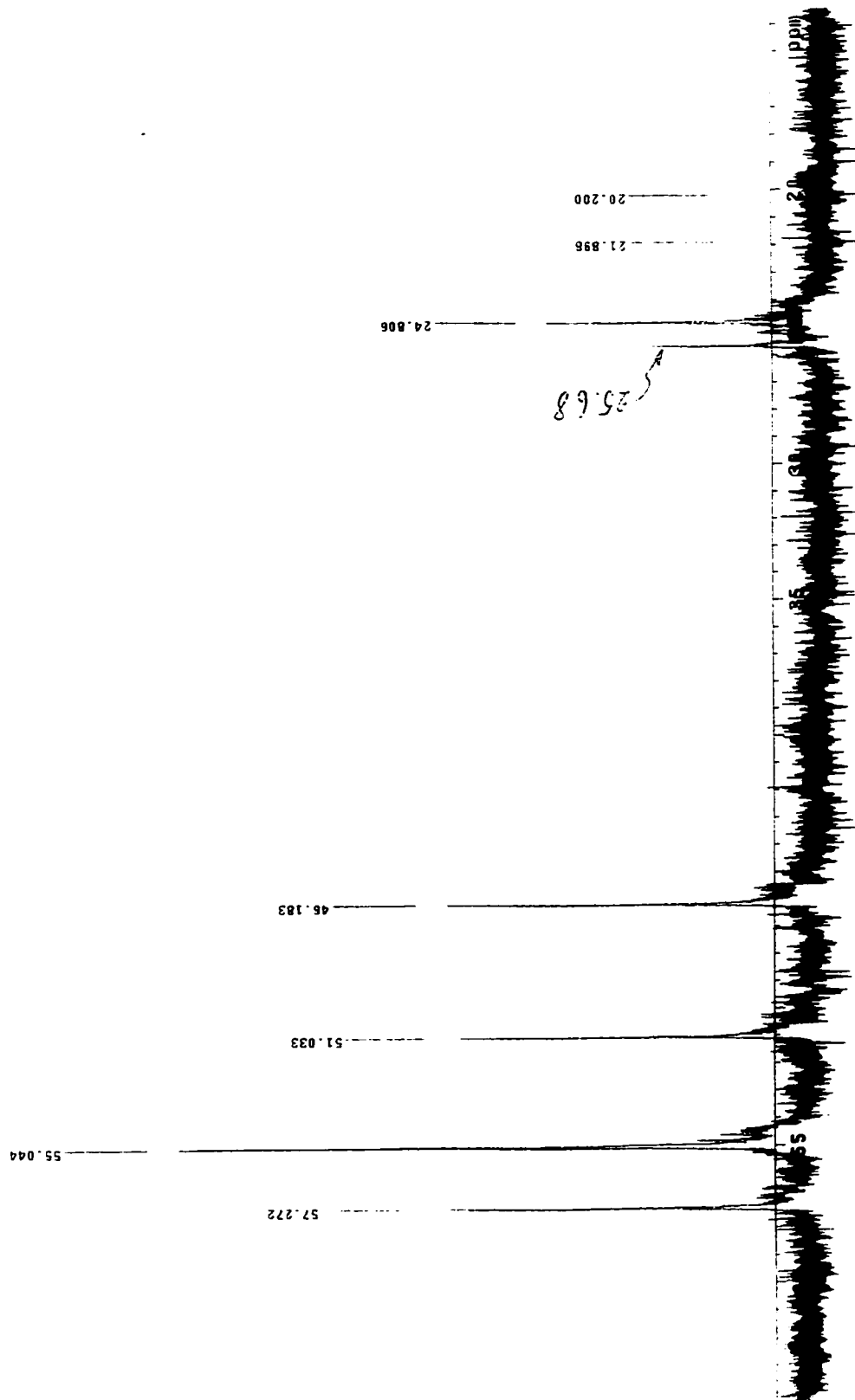




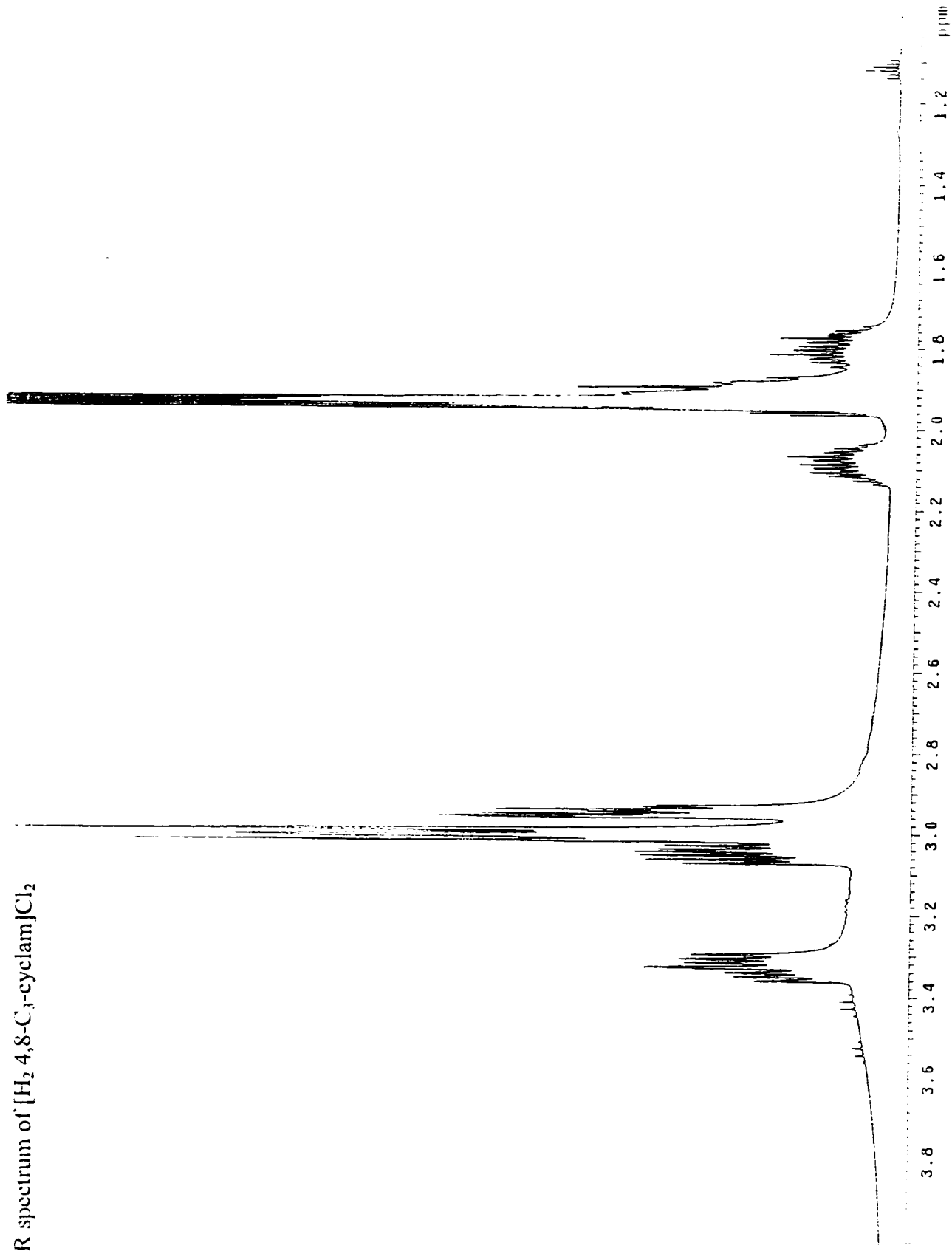
$^1\text{H}$  NMR spectrum of  $[\text{H}_2\text{ 4,8-C}_3\text{-cyclam}](\text{ClO}_4)_2$



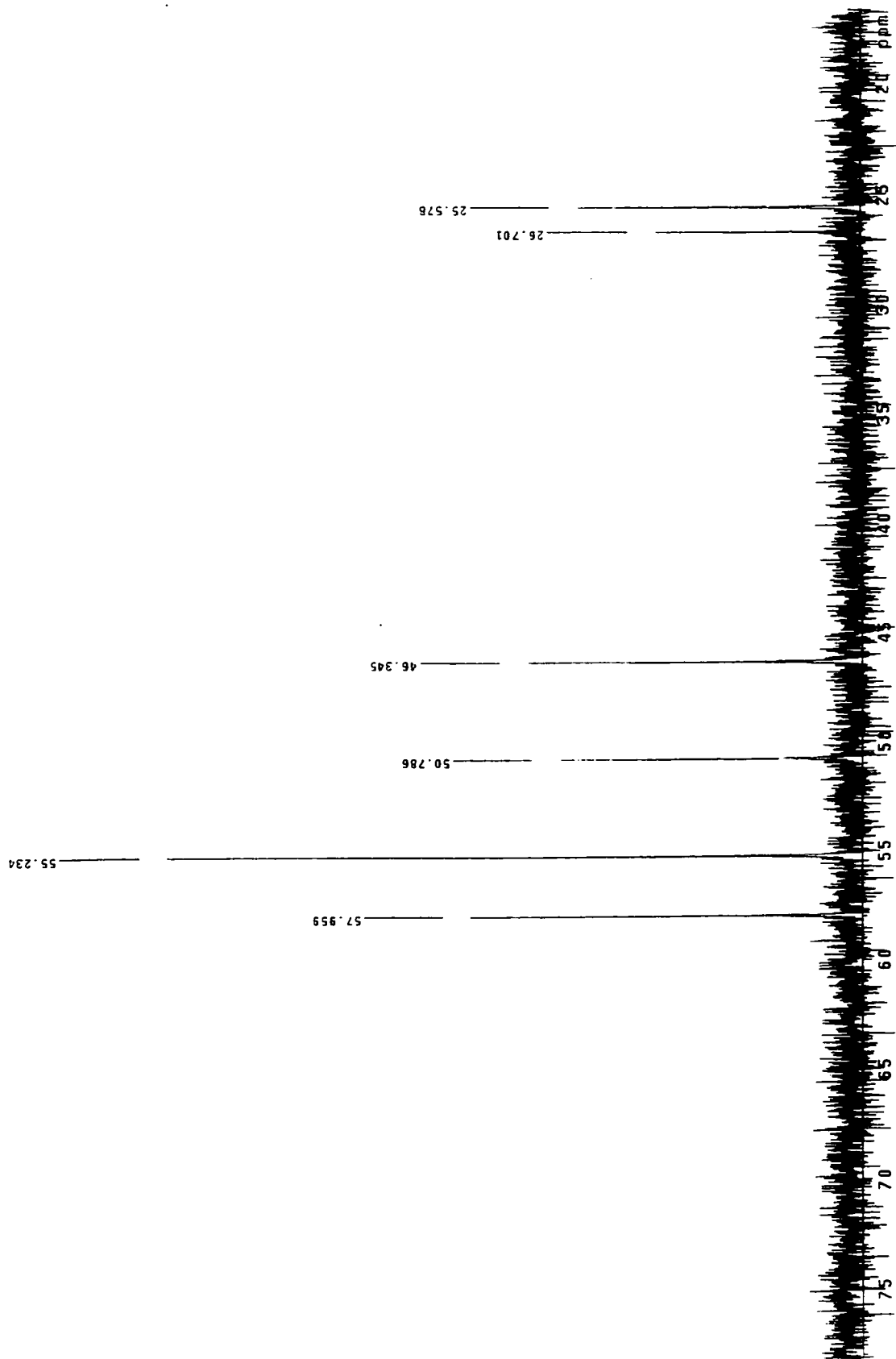
$^{13}\text{C}$  NMR spectrum of  $[\text{H}_2\text{4,8-C}_3\text{-cyclam}](\text{ClO}_4)_2$



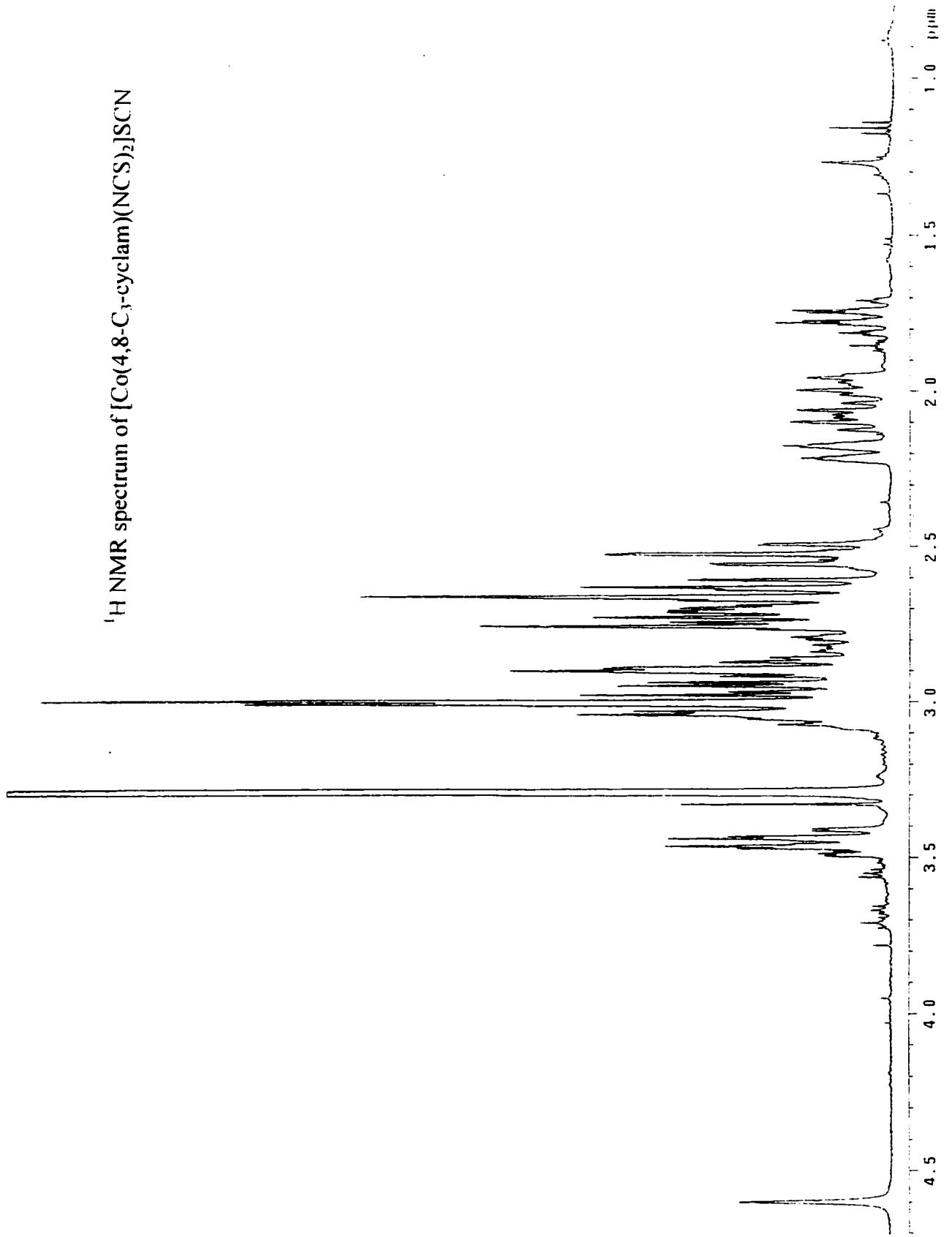
<sup>1</sup>H NMR spectrum of [H<sub>2</sub> 4,8-C<sub>3</sub>-cyclam]Cl<sub>2</sub>



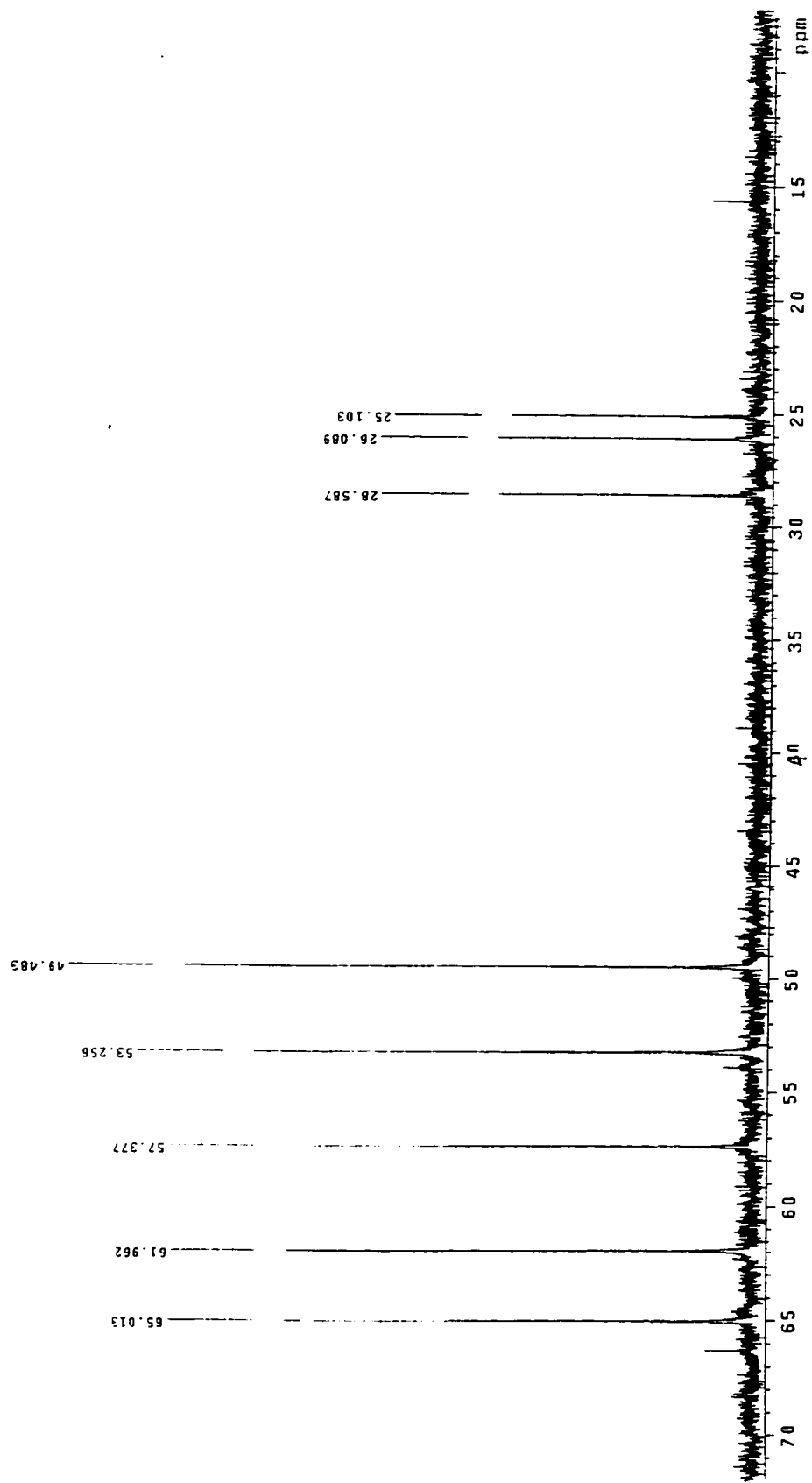
$^{13}\text{C}$  NMR spectrum of  $[\text{H}_2\text{ 4,8-C}_3\text{-cyclam}]\text{Cl}_2$



$^1\text{H}$  NMR spectrum of  $[\text{Co}(4,8\text{-C}_3\text{-cyclam})(\text{NCS})_2]\text{SCN}$



$^{13}\text{C}$  NMR spectrum of  $[\text{Co}(4,8\text{-C}_3\text{-cyclam})(\text{NCS})_2]\text{SCN}$



Crystal structure of [Co(1,11-C<sub>3</sub>-cyclam)(NCS)<sub>2</sub>]OTf

